Bell correlation depth in many-body systems

F. Baccari,[1] J. Tura,[1,2] M. Fadel,[3] A. Aloy,[1] J.-D. Bancal,[3] N. Sangouard,[3] M. Lewenstein,[1,4] A. Acín,[1,4] and R. Augusiak[5]
[1]Institut de Ciencies Fotoniques (ICFO), Barcelona Institute of Science and Technology, 08860 Castelldefels (Barcelona), Spain
[2]Max-Planck-Institut für Quantenoptik, Hans-Kopfermann-Straße 1, 85748 Garching, Germany
[3]Department of Physics, University of Basel, Klingelbergstrasse 82, 4056 Basel, Switzerland
[4]ICREA, Passeig Lluis Companys 23, 08010 Barcelona, Spain
[5]Center for Theoretical Physics, Polish Academy of Sciences, Aleja Lotników 32/46, 02-668 Warsaw, Poland

(Received 22 March 2019; published 22 August 2019)

We address the question of assessing the number of particles sharing genuinely nonlocal correlations in a multipartite system. While the interest in multipartite nonlocality has grown in recent years, its existence in large quantum systems is difficult to confirm experimentally. This is mostly due to the inadequacy of standard multipartite Bell inequalities to many-body systems: Such inequalities usually rely on expectation values involving many parties, usually all, and require individual addressing of each party. In addition, known Bell inequalities for genuine nonlocality are composed of a number of expectation values that scales exponentially with the number of observers, which makes such inequalities impractical from the experimental point of view. In a recent work [Tura *et al.*, Science **344**, 1256 (2014)], it was shown that it is possible to detect nonlocality in multipartite systems using Bell inequalities with only two-body correlators. This opened the way for the detection of Bell correlations with trusted collective measurements through Bell correlation witnesses [Schmied *et al.*, Science **352**, 441 (2016)]. These witnesses were recently tested experimentally in many-body systems such as Bose-Einstein condensate or thermal ensembles, hence demonstrating the presence of Bell correlations with assumptions on the statistics. Here, we address the problem of detecting nonlocality depth, a notion that quantifies the number of particles sharing nonlocal correlation in a multipartite system. We introduce a general framework allowing us to derive Bell-like inequalities for nonlocality depth from symmetric two-body correlators. We characterize all such Bell-like inequalities for a finite number of parties and we show that they reveal Bell correlation depth $k \leqslant 6$ in arbitrarily large systems. We then show how Bell correlation depth can be estimated using quantities that are within reach in current experiments. On one hand, we use the standard multipartite Bell inequalities such the Mermin and Svetlichny ones to derive Bell correlations witnesses of any depth that involves only two collective measurements, one of which being the parity measurement. On the other hand, we show that our two-body Bell inequalities can be turned into witnesses of depth $k \leqslant 6$ that require measuring total spin components in certain directions. Interestingly, such a witness is violated by existing data from an ensemble of 480 atoms.

DOI: 10.1103/PhysRevA.100.022121

I. INTRODUCTION

Local measurements on composite quantum systems may lead to fascinating correlations that cannot be explained by any local realistic theory such as classical physics. This phenomenon, usually referred to as nonlocality (cf. Ref. [1]), proves that the laws of physics at the microscale significantly differ from those at the macroscale. More important, in recent years it has been understood that nonlocality is a powerful resource for device-independent applications that have no classical analog, with the most prominent examples being device-independent quantum key distribution [2,3], device-independent entanglement detection [4,5], generation and amplification of randomness [6–8], and self-testing [9].

However, to be able to fully exploit nonlocality as a resource, one first needs efficient methods to detect it in the composite quantum systems that can exhibit it. Since these systems can produce nonlocality upon measurement, i.e., statistics violating a Bell inequality [10], we say that their state is Bell correlated. Bell inequalities are naturally the most common tool of revealing both nonlocal statistics and Bell correlated states. These are inequalities constraining the set of local realistic correlations, and their violation signals nonlocality. A considerable amount of effort has been devoted to introduce various constructions of Bell inequalities [11]. Still, the problem of nonlocality detection is much less advanced in the multipartite case than in the bipartite one, in which recently loophole-free Bell tests have been performed [12–15] and pushed to ever-higher standards [16–21]. There are two main reasons for that: (i) The mathematical complexity of finding all Bell inequalities grows double exponentially with the number of parties and (ii) experimental verification of nonlocality is much more demanding in the multipartite case; in particular, individual settings assignments for each party are needed to test a Bell inequality, and most of the known multipartite Bell inequalities (such as, for instance, the Mermin Bell inequality) involve a large number of measurements and are constructed from correlation functions involving measurements by all parties (see Ref. [11]). Therefore, such inequalities are not suited to detect nonlocal correlations in many-body systems in which only a few collective measurements can be applied and one typically has access only to two-body correlations.

One of the ways to tackle these difficulties in the multipartite case, recently put forward in Refs. [22,23], is to consider Bell inequality involving only two-body correlators. This reduces the mathematical complexity of the problem and allowed demonstration that these inequalities are powerful enough to reveal nonlocality in composite quantum systems with an arbitrary number of particles [24–27]. Moreover, these inequalities can be used to derive Bell correlation witnesses expressed in terms of just a small number of collective two-body expectation values, which are routinely measured in certain many-body quantum systems (see Refs. [28,29]). This makes these witnesses very practical and allowed testing them in two experiments recently reporting on Bell correlations in Gaussian many-body states consisting of 480 atoms [23] in a Bose-Einstein condensate and 5×10^5 particles [30] in a thermal ensemble.

However, the violation of these Bell inequalities and the corresponding witnesses only signals the presence of some kind of Bell correlations. In fact, it is unable to provide more quantitative information about it. This naturally raises the question of how to reveal the depth of nonlocality in many-body systems, that is, how many particles share genuine Bell correlations. At first sight, the problem is challenging. Known Bell inequalities for genuine nonlocality not only use expectation values involving all parties but also require the ability to perform a different measurement on each party. Furthermore, the number of measurement settings scales exponentially with the number of parties.

The main aim of this work is to address this question. We first introduce a general framework to study the problem of revealing the nonlocality depth in multipartite systems using two-body correlations only, hence guaranteeing that no high-order moment will be necessary at the level of the witness. The problem of detection of genuine nonlocality in this context is fully characterized for a relatively small number of parties, providing lists of Bell-like inequalities that do the job. Moreover, we give a Bell-like inequality detecting the nonlocality depth from 1 to 7 for any number of parties. We then turn to the question of witnessing Bell correlations depth in many-body systems. First, building on the Mermin and Svetlichny inequalities, we show that the nonlocality depth of any multipartite system can be tested via a Bell correlation witness, using only two trusted collective measurements. This gives access to genuine Bell correlations in many-body systems where one high-order measurement can be performed. Lastly, we derive witnesses corresponding to the two-body Bell inequalities we found and we apply them to detect the Bell correlations depth of a Bose-Einstein condensate with 480 atoms.

This work is structured as follows: In Sec. II, we introduce all the concepts relevant to make this work self-contained. In particular, we discuss the Bell scenario and correlations in Sec. II A and the concepts of k-producibility of correlations in Sec. II B. In Sec. III, we formally state the main results of our work. In Sec. IV, we characterize the sets of k-producible correlations with two-body correlators. In particular, in Sec. IV A, we characterize the vertices of the polytope of k-producible two-body symmetric correlations, and in Sec. IV B, we describe the procedure to project the nonsignalling polytope. In Sec. V, we present classes of Bell-like inequalities for nonlocality depth, built from two-body correlations. In Sec. VI, we discuss the experimental aspects of witnessing k-body Bell correlations. In particular, we show how genuine nonlocality can be witnessed from Svetlichny and Mermin inequalities in Sec. VI A, and in Sec. VI B, we show how to construct the witness for Bell inequalities that involve only two-body correlations. We conclude in Sec. VII.

This work contains six technical appendices. In Appendix A, we recall the basic definitions and properties of polytopes that are used in our work. In Appendix B, we describe in detail the projection of the vertices of k-producible polytopes. In Appendix D, we present the vertices of the projected nonsignalling polytopes for $k = 2, 3, 4$. In Appendix E, we provide a complete list of facets of two-body symmetric polytopes that test for genuine nonlocality up to five parties. In Appendix F, we present the technical derivation of an inequality for k-nonlocality depth valid for any number of parties. Finally, in Appendix G, we estimate the Svetlichny and Mermin operators with collective spin measurements.

II. PRELIMINARIES

In this section, we review the concepts and background information that are necessary to properly introduce our results in Sec. III. We focus on the Bell scenario and correlations in Sec. II A and on the notions of k-producibility of nonlocality, nonlocality depth, and genuine nonlocality in Sec. II B.

A. Bell scenario and correlations

Consider N separated parties denoted $A_1, \dots, A_N$ sharing some N-partite physical system. Each party is allowed to perform measurements on their share of this system and each party will obtain the corresponding outcome. Here we consider the simplest scenario in which party A_i has two observables at their disposal, denoted $M^{(i)}_{x_i}$ with $x_i = 0, 1$, and each observable is assumed to yield one out of two possible outcomes $a_i = \pm 1$. Such a scenario is generally referred to as the $(N, 2, 2)$ scenario (i.e., N parties, 2 measurements, 2 outcomes). In a Bell experiment, measurements are repeated many times, after which the parties estimate the conditional probabilities $p(a_1, \dots, a_N|x_1, \dots, x_N) \equiv p(\mathbf{a}|\mathbf{x})$ of obtaining outcomes $a_1, \dots, a_N =: \mathbf{a}$ upon performing the measurements labeled by $x_1, \dots, x_N =: \mathbf{x}$. Therefore, the available information is summarized in a collection of these probabilities $\{p(\mathbf{a}|\mathbf{x})\}$. Clearly, $\{p(\mathbf{a}|\mathbf{x})\}$ cannot be an arbitrary list of numbers; the numbers $p(\mathbf{a}|\mathbf{x})$ need to be non-negative and normalized for any choice of inputs $\mathbf{x}$ in order to be, at least, mathematically consistent.

From a physical point of view, it is then natural to assume that the probabilities $p(\mathbf{a}|\mathbf{x})$ must fulfill, in addition, the *no-signaling principle*; i.e., the choice of measurement of the kth party cannot influence the outcome of the remaining measurements. Mathematically, this is represented by imposing the following conditions:

$$\sum_{a_i}[p(a_1,\ldots,a_i,\ldots,a_N|x_1,\ldots,x_i,\ldots,x_N) - p(a_1,\ldots,a_i,\ldots,a_N|x_1,\ldots,x_i',\ldots,x_N)] = 0, \quad (1)$$

for all x_i, x_i', $a_1,\ldots,a_{i-1},a_{i+1},\ldots,a_N$ and $x_1,\ldots,x_{i-1},x_{i+1},\ldots,x_N$ and all $i = 1,\ldots,N$. The probabilities that obey the no-signaling principle are commonly referred to as the *no-signaling correlations*. Interestingly, these correlations form a polytope, that is, a convex set defined by a finite amount of linear inequalities (see Appendix A for more details). We denote such a polytope $\mathcal{NS}_N$ and we refer to it as the no-signaling polytope. Note that $\mathcal{NS}_N$ results from the intersection of the set satisfying the inequalities $p(\mathbf{a}|\mathbf{x}) \geqslant 0$ with the normalization and no-signaling constraints (1).

Consider now the correlations that arise by performing local measurements on some quantum state ρ_N. The resulting probabilities are expressed via the Born rule as

$$p(a_1,\ldots,a_N|x_1,\ldots,x_N) = \mathrm{Tr}\big(\rho_N M_{x_{i_1}}^{a_1}\otimes\cdots\otimes M_{x_{i_N}}^{a_N}\big), \quad (2)$$

where $M_{x_{i_i}}^{a_i} \succeq 0$ denote the measurement operators, represented by positive-operator valued measures (POVMs) satisfying the normalisation condition $\sum_{a_i} M_{x_{i_i}}^{a_i} = \mathbb{I}$ (forming a resolution of the identity). It turns out that the set of all *quantum correlations*, denoted $\mathcal{Q}_N$, is also convex if no assumption on the local dimension of the state used in the experiment is made.

Another relevant notion is the one of *local correlations*, which consists of those probabilities that can be obtained by the parties when the only resource they share is classical information, represented by some random variable λ with a probability distribution p_λ. The most general form of such correlations is (cf. also Refs. [1,31])

$$p(a_1,\ldots,a_N|x_1,\ldots,x_N) = \sum_\lambda p_\lambda \prod_{i=1}^N p(a_i|x_i,\lambda). \quad (3)$$

The set that correlations of the form (3) define is also a polytope, which we denote as $\mathcal{P}_N$, and we refer to as the local polytope. Recall that a polytope can be equivalently represented by a finite number of vertices (see also Appendix A for a more formal definition). The vertices of $\mathcal{P}_N$ are of special interest, as they correspond to the case that $p(a_i|x_i,\lambda) = D(a_i|x_i,\lambda)$, where for a given λ, $D(a_i|x_i,\lambda)$ is a deterministic function returning some a_i with probability 1 for each x_i. Therefore, vertices of the local polytope correspond to local deterministic strategies.

The corresponding linear inequalities enclosing the local polytope are the so-called Bell inequalities. As first shown by Bell [10], there are quantum correlations that violate Bell inequalties and hence do not admit a decomposition of the form (3). We call such correlations nonlocal and, in the case that these correlations were obtained from a quantum state ρ, we say that this state displays Bell correlations. Note that no-signaling correlations can generally violate Bell inequalities more than quantum correlations do, meaning that there are probabilities satisfying the no-signaling principle that do not have a quantum representation [32]. Therefore, the relations between the three sets introduced above can be summarized as $\mathcal{P}_N \subset \mathcal{Q}_N \subset \mathcal{NS}_N$, where both inclusions are strict.

To conclude, it is useful to notice that in the simplest scenario of each party performing dichotomic measurements, correlations can be equivalently described by a collection of expectation values

$$\big\{\big\langle M_{x_{i_1}}^{(i_1)}\ldots M_{x_{i_k}}^{(i_k)}\big\rangle\big\}_{i_1,\ldots,i_k;x_{i_1},\ldots,x_{i_k};k}, \quad (4)$$

with $i_1 < \cdots < i_k = 1,\ldots,N$ and $k = 1,\ldots,N$ (all possible expectation values, ranging from the single-body to N-partite ones are taken into account). The probability and correlator representations are related through the formula

$$p(\mathbf{a}|\mathbf{x}) = \frac{1}{2^N}\left[1+\sum_{k=1}^N \sum_{1\leqslant i_1<i_2<\ldots<i_k\leqslant N} a_{i_1}\ldots a_{i_k}\big\langle M_{x_{i_1}}^{(i_1)}\ldots M_{x_{i_k}}^{(i_k)}\big\rangle\right] \quad (5)$$

that holds for any $\mathbf{a}, \mathbf{x}$. The main advantage of the correlator picture is that it automatically incorporates the no-signaling constraints, thus reducing the number of variables that need to be considered. In particular, this implies that the no-signaling set can be simply described by the conditions of non-negativity of probabilities $p(a_1,\ldots,a_N|x_1,\ldots,x_N) \geqslant 0$, expressed in terms of correlators through (5). Notice also that although we stated all the above definitions in terms of probabilities, everything can be reformulated in correlator form, by directly applying the Fourier transform (5).

B. The concepts of *k*-producibility of nonlocality and nonlocality depth

As already said, violation of standard Bell inequalities signals nonlocality, i.e., the impossibility of representing the observed statistics in the form of (3). However, in the multipartite scenario, this tells us nothing about how many parties share genuine nonlocal correlations. To give an illustrative example, imagine a tripartite distribution that factorizes in the following form $p(a_1a_2|x_1x_2)p(a_3|x_3)$: If the correlations shared between the first two particles are nonlocal, clearly the whole distribution is also classified as nonlocal. Nonetheless, one can intuitively see that this is a "weak" form of nonlocality for a tripartite scenario, given that the set of particles sharing nonlocal correlations is only bipartite.

Several approaches have been proposed to describe the types of nonlocality that can appear in such a scenario [33,34]. Following Ref. [34], we choose here the notion of k-producibility of nonlocality or nonlocality depth, which goes along the lines developed to describe mutipartite entanglement, although the nonlocality case entails much subtler differences (see Refs. [35–37]). We are thus interested in quantifying the number of parties that share genuinely nonlocal correlations. To this end, we partition the set $I = \{1,\ldots,N\}$ into L pairwise disjoint nonempty subsets $\mathcal{A}_i$, such that by joining them one recovers I and the size of each $\mathcal{A}_i$ is at most k parties. We denote such a partition an L_k partition of I. Consider now correlations that admit the following decomposition:

$$p(\mathbf{a}|\mathbf{x}) = \sum_\lambda p(\lambda)p_1(\mathbf{a}_{\mathcal{A}_1}|\mathbf{x}_{\mathcal{A}_1},\lambda)\times\cdots\times p_L(\mathbf{a}_{\mathcal{A}_L}|\mathbf{x}_{\mathcal{A}_L},\lambda), \quad (6)$$

where $\mathbf{a}_{\mathcal{A}_i}$ and $\mathbf{x}_{\mathcal{A}_i}$ are vectors encoding the outcomes and measurement choices corresponding to the observers belonging to $\mathcal{A}_i$. We call such correlations k-producible with respect to the above partition of I. One can see that this is a natural generalization of the tripartite example given above, where now the largest number of particles sharing nonlocal correlations is defined by the size of the largest subset $\mathcal{A}_i$, hence k.

We choose the nonlocal resources shared by the parties to be no-signalling correlations, that is, we require the distributions $p_i(\mathbf{a}_{\mathcal{A}_i}|\mathbf{x}_{\mathcal{A}_i}, \lambda)$ to satisfy the no-signalling conditions (1). Apart from a physical motivation, this is done also in order to avoid describing a self-contradicting model [36,37]. It is worth noting that the choice of no-signaling resources is not the only possibility that avoids inconsistencies: One could also make the more restrictive assumption that all $p_i(\mathbf{a}_{\mathcal{A}_i}|\mathbf{x}_{\mathcal{A}_i}, \lambda)$ are quantum correlations, which we have explored in a different work [38], yielding device-independent witnesses of entanglement depth in this case.

Still, the form of correlations (6) is not yet the most general one as by mixing correlations (6) that are k-producible with respect to different L_k partitions of I, one cannot increase the nonlocality depth of the resulting probability distribution. To be more precise, denote by S_k the set of all possible L_k-partitions of I, where the number L of subsets $\mathcal{A}_i$ is allowed to vary but k is fixed. We then call correlations $\{p(\mathbf{a}|\mathbf{x})\}$ *k-producible* if they can be written as the following convex combination:

$$p(\mathbf{a}|\mathbf{x}) = \sum_{L_k \in S_k} q_{L_k} p_{L_k}(\mathbf{a}|\mathbf{x}), \tag{7}$$

where $p_{L_k}(\mathbf{a}|\mathbf{x})$ are correlations that admit the decomposition (6) with respect to a given k partition L_k. The minimal k for which a distribution can be expressed in the form (7) is called the *nonlocality depth*.[1] Equivalently, correlations whose nonlocality depth is k are generally referred to as *genuinely k-partite nonlocal* or, simply, *k-nonlocal* [39]. Generalizing the notion introduced in the previous section, we also say that a state capable of generating k-nonlocal correlations displays a *Bell correlations depth* of k.

Let us also notice that in the particular case of $k = 1$, where each party forms a singleton $\mathcal{A}_i = \{A_i\}$ $(i = 1, \dots, N)$, one recovers the above introduced definition of local correlations (3). Then, on the other extreme $k = N$, we have correlations in which all parties share nonlocality and are thus called genuinely multipartite nonlocal (GMNL).

Geometrically, as in the case of fully local models (3), k-producible correlations form polytopes, denoted $\mathcal{P}_{N,k}$. Similar to the local polytope, vertices of these polytopes are product probability distributions of the form

$$p(\mathbf{a}|\mathbf{x}) = p_1(\mathbf{a}_{\mathcal{A}_1}|\mathbf{x}_{\mathcal{A}_1}) \times \cdots \times p_L(\mathbf{a}_{\mathcal{A}_L}|\mathbf{x}_{\mathcal{A}_L}), \tag{8}$$

with each $p_i(\mathbf{a}_{\mathcal{A}_i}|\mathbf{x}_{\mathcal{A}_i})$ being a vertex of the corresponding $|\mathcal{A}_i|$-partite nonsignaling polytope (or, when $|\mathcal{A}_i| = 1$, a deterministic vertex $D(a_i|x_i)$ of the local polytope). One then needs to consider all L_k partitions in order to construct all vertices of $\mathcal{P}_{N,k}$: Different elements $S \in S_k$ yield different factorizations (8) and, therefore, different sets of vertices. It thus follows that the necessary ingredient in order to construct all vertices of $\mathcal{P}_{N,k}$ are the vertices of the p-partite nonsignaling polytopes $\mathcal{NS}_p$ for all $p \leqslant k$.

Let us also notice that, with the aid of the formula (5), all the above definitions can be equivalently formulated in terms of correlators (4); in particular, for a vertex (8) the correlators (4) factorize whenever the parties belong to different groups $\mathcal{A}_i$.

The facets constraining the $\mathcal{P}_{N,k}$ polytopes can also be interpreted as Bell-like inequalities. In this case, the violation of such inequalities implies that a given distribution cannot be described by any k-producible model. Hence, it certifies that the observed correlations are at least $(k+1)$ nonlocal. In order to quantify the nonlocality depth of corrleations, these are the families of inequalities that we are interested in characterizing. In the following section, we start by summarizing the techniques we use and our main results.

III. STATEMENT OF THE MAIN RESULTS

The main objective of this work is to provide efficient tools to assess the nonlocality depth of multipartite systems. As we explained in Sec. II, to study nonlocality depth in full generality one needs to characterize the polytopes of k-producible correlations, denoted $\mathcal{P}_{N,k}$, for any number of particles N and nonlocality depth k. However, to successfully address this problem, one needs to overcome two major obstacles.

First, despite the general form of the vertices of $\mathcal{P}_{N,k}$ [cf. (8)], constructing them in practice requires previous knowledge about *all* the vertices of the no-signaling polytopes $\mathcal{NS}_p$ for $p \leqslant k$, whose determination is already a formidable task. Indeed, while the facets of the no-signaling polytopes are easy to enumerate for any number of particles, its complete list of vertices has been derived only in the simplest scenarios of $N = 2, 3$ [40]. It should also be mentioned that in Ref. [41] a polyhedral duality between Bell inequalities and the vertices of the nonsignaling polytope in the $(N, 2, 2)$ scenario was established, thus proving that finding all vertices of $\mathcal{NS}_p$ is equivalent to find all tight Bell inequalities in $\mathcal{P}_p$. The difficulty in finding all Bell inequalities in a given scenario was already observed by Pitowsky [42], and it was later proven to be NP hard even in a bipartite setting [43].

Second, suppose one could actually list all the extremal points of $\mathcal{P}_{N,k}$. The size of this list would grow exponentially as a function of N: Simply consider the L_k partition consisting of the maximal amount of subsets of size k (plus a smaller subset if k does not divide N). Then, by denoting v_k as the number of vertices of $\mathcal{NS}_k$, we see from (8) that the number of vertices of $\mathcal{P}_{N,k}$ will grow as $O(v_k^{\lfloor N/k \rfloor})$. This exponential growth with N already renders any effort to derive a complete list of Bell inequalities for nonlocality depth for large values of N futile.

To overcome these difficulties, we restrict our analysis to the scenario of symmetric two-body correlations, first

[1] A more adequate terminology would be *nonlocality depth with respect to nonsignaling resources* or simply *NS nonlocality depth* as in the definition of k-producibility we assume the probabilities $p_i(\mathbf{a}_{\mathcal{A}_i}|\mathbf{x}_{\mathcal{A}_i}, \lambda)$ to be nonsignaling, whereas according to Refs. [36,37] other types of resources can also be considered.

introduced in Ref. [22]. Hence, instead of working with the full probability distribution $p(a_1,\dots,a_N|x_1,\dots,x_N)$, we imagine that the only accessible information consists of the following one- and two-body expectation values:

$$\langle M_x^{(i)}\rangle, \qquad \langle M_x^{(i)}M_y^{(j)}\rangle \tag{9}$$

with $i\neq j=1,\dots,N$ and $x,y=0,1$. Such an assumption is particularly relevant for experimental applications, since those quantities can be efficiently estimated with just a polynomial amount of measurements. In addition, this allows us to answer a fundamental question: whether two-body correlators, i.e., the minimal amount of information needed to detect nonlocality in a quantum system, are enough to reveal nonlocality depth in a multipartite system. Moreover, we look for Bell inequalities that are invariant under an exchange of any pair of parties, meaning that they are function of the symmetrized quantities

$$\mathcal{S}_x := \sum_{i=1}^{N}\langle M_x^{(i)}\rangle, \quad \mathcal{S}_{xy} := \sum_{\substack{i,\,j=1\\ i\neq j}}^{N}\langle M_x^{(i)}M_y^{(j)}\rangle \tag{10}$$

with $x,y=0,1$. Mathematically, this implies that instead of studying the full $\mathcal{P}_{N,k}$ polytope, we want to characterize its projection $\mathcal{P}_{N,k}^{2,S}$ onto the lower dimensional space of symmetric one- and two-body correlators, spanned by the five quantities (10) [44].

Therefore, we look for a complete characterization of the symmetric two-body Bell inequalities that detect nonlocality depth, whose most general form is

$$I := \alpha\mathcal{S}_0+\beta\mathcal{S}_1+\frac{\gamma}{2}\mathcal{S}_{00}+\delta\mathcal{S}_{01}+\frac{\varepsilon}{2}\mathcal{S}_{11}+\beta_k \geqslant 0, \tag{11}$$

with

$$\beta_k = -\min_{\mathcal{P}_{N,k}^{2,S}} I, \tag{12}$$

where the minimum is taken over all correlations belonging to $\mathcal{P}_{N,k}^{2,S}$.

Recall that the case of $k=1$ recovers the study of the local polytope, whose complete list of Bell inequalities is unknown already for $N\geqslant 4$. Interestingly, it turns out that restricting to its symmetric two-body projection dramatically simplifies the problem, as was extensively shown in Refs. [22,24,44]. More precisely, such a projection makes it possible to derive all the facets of the local polytope for scenarios with tens of particles, which allowed also to introduce classes of inequalities valid for any N.

Here, we take a step forward and look at the cases corresponding to $k>1$. Remarkably, we see that many simplifications can be carried out in the generic nonlocality depth case as well. The rest of the section is devoted to briefly summarizing our results, as well as their applications to the study of correlations in many-body systems, while leaving the in-depth presentation to Secs. IV, V, and VI.

Result 1. The vertices of the polytopes $\mathcal{P}_{N,k}^{2,S}$ can be computed efficiently as functions of the vertices of the projected no-signaling polytopes $\mathcal{NS}_p^{2,S}$ of $p\leqslant k$ parties. For a fixed value of k, the number of vertices scales polynomially with N.

Recall the first obstacle stated above, regarding the complexity of finding the vertices of $\mathcal{NS}_N$ for a general N. Our first result implies that, in order to study nonlocality depth with symmetric two-body correlators, it is not necessary to find all the vertices of $\mathcal{NS}_N$, and it is sufficient to find the vertices of its projection to the two-body symmetric subspace, $\mathcal{NS}_N^{2,S}$.

Note, however, that determining the projection of a polytope is not a simple task, especially if the original polytope is described in terms of inequalities, which is the case for $\mathcal{NS}_N$. The general procedure to find such a projection relies on the Fourier-Motzkin elimination method (see Appendix A), which has an exponential scaling with the number of components that need to be projected out (note that the number of correlators involving more than two parties already scales exponentially with N, therefore yielding an overall doubly exponential scaling). Indeed, the $\mathcal{NS}_N$ polytope is parametrized by the correlators (4), and there are 3^N-1 of them, while $\mathcal{NS}_N^{2,S}$ is embedded in a five-dimensional space for any N [cf. (11)]; therefore, applying Fourier-Motzkin is basically impractical for any $N>2$.

Nonetheless, in Sec. IV, we show that the structure of the no-signaling polytope can be exploited to dramatically reduce the complexity of the problem. In particular, we divide the projection operation into two steps: first, the symmetrization one, which yields the polytope $\mathcal{NS}^S$, parametrized by the symmetric correlators (10) of any order, and second, the projection onto the two-body space $\mathcal{NS}^{2,S}$, which consists in removing all the symmetric correlators of order higher than 2. By following this procedure, we arrive at our second result, which is the technical key point of our work:

Result 2. The facets of the $\mathcal{NS}_N^S$ polytopes can be efficiently obtained for any N. Then, the projection operation to get the desired $\mathcal{NS}_N^{2,S}$ polytopes involve projecting out a number of components that scales only as $O(N^2)$.

Combining the two results, we are able to make several advancements in the problem of detecting nonlocality depth in multipartite systems. Thanks to Result 2, we are able to obtain the complete list of vertices of the $\mathcal{NS}_N^{2,S}$ polytopes for up to $N=6$ parties. This allows us to characterize the vertices of the polytopes of k-producible correlations for a nonlocality depth of $k\leqslant 6$. Because of the exponential reduction with respect to Result 1, it is then possible to obtain all the Bell inequalties detecting such nonlocality depths for systems of $N\leqslant 15$ particles. In Sec. V, we present the main findings regarding those inequalities, among others the possibility of efficiently detecting GMNL up to seven parties.

Moreover, we study a class of Bell inequalities, valid for any N, whose k-producible bound β_k varies with k and is violated by quantum correlations for sufficiently large N if $k\leqslant 6$. This leads to our third result:

Result 3. Nonlocality depth, for values of at least $k\leqslant 6$, can be detected with symmetric two-body correlators in systems composed of any number of particles.

Up to now, all the results we have presented are purely device independent. Therefore, if one were capable of performing a loophole-free Bell test [12–21] among the involved parties, one would be able to certify the aforementioned nonlocality depth of the correlations being produced. However, two-body permutationally invariant Bell inequalities have an additional extra feature: They can be used to construct quantum operators that can always be evaluated with only first and second moments of collective observables [22]. When the measurements are trusted, these operators act as witnesses for states that can display Bell correlation depth k, i.e., entangled states capable of producing k-nonlocal correlations [23]. This makes it possible to see if Bell correlations with higher nonlocality depth arise naturally in low-energy states of many-body systems [26,45,46]. In Sec. VI, we turn our attention toward the application of our findings to the study of many-body systems. Importantly, in such a scenario, the information accessible is often represented by collective observables, which are enough to estimate the expectation values of Bell correlation witnesses.

Notice that thus far Bell correlation witnesses have been studied only in the context of two-body inequalities detecting standard nonlocal correlations. We first consider their application to already known full-body Bell inequalities capable of distinguishing nonlocality depth, such as the Mermin [47] and Svetlichny inequalities [39]. In Sec. VI A, we show that, although being composed by an exponentially large number of terms, such inequalities can be related to witnesses involving only two collective measurements. This is our fourth result:

Result 4. Bell correlation depth up to $k = N$ can be detected for all N with a witness involving only two collective measurements.

The ability to detect large Bell correlation depths through the collective witnesses issued from the Svetlichny and Mermin inequalities comes at the price that one of these collective observables consists in a parity measurement, which is technologically demanding in large systems. This motivates us to turn our attention to the Bell correlation witnesses that can be constructed with the two-body Bell inequalities introduced here. In particular, we connect the class of Bell inequalities studied in Sec. V to witnesses related to the squeezing parameter in a many-body state. We conclude by applying this witness to already available experimental data from a Bose-Einstein condensate to show the following:

Result 5. Entangled k-nonlocal states, for values of at least $k \leqslant 6$, can be detected in many-body systems of in principle any number of particles.

We devote the rest of the paper to presenting our results in detail.

IV. CHARACTERIZING THE SETS OF k-PRODUCIBLE CORRELATIONS WITH TWO-BODY CORRELATORS

Our aim in this section is characterization of the symmetric two-body polytopes of k-producible correlations $\mathcal{P}_{N,k}^{2,S}$ defined in Sec. II B. To this end, we will also determine the vertices of the projections of the nonsignaling polytopes onto two-body symmetric correlations $\mathcal{NS}_N^{2,S}$ for small values of N.

A. Characterization of the vertices of the k-producible two-body symmetric polytopes

Here, we introduce a general description of all the vertices of the projected $\mathcal{P}_{N,k}^{2,S}$ polytopes. This description assumes previous knowledge of all the vertices of the symmetrized p-partite no-signaling polytope $\mathcal{NS}_p^{2,S}$ for each $p \leqslant k$.

Let us introduce the following notation. Let n_p be the number of vertices of $\mathcal{NS}_p^{S,2}$, with $1 \leqslant p \leqslant k$. We want to compute the values that the correlators (10) take in the ith vertex, with $1 \leqslant i \leqslant n_p$. Let $\vec{S}(p,i)$ denote the five-dimensional vector

$$\vec{S}(p,i) = [S_0(p,i), S_1(p,i), S_{00}(p,i), S_{01}(p,i), S_{11}(p,i)] \tag{13}$$

of one- and two-body symmetric expectation values for the ith vertex of $\mathcal{NS}_p^{2,S}$. We denote by $\{\vec{S}(p,i)\}_{p,i}$ the list of all such five-dimensional vectors (13).

Each vertex of the two-body symmetric polytope of k-producible correlations $\mathcal{P}_{N,k}^{2,S}$ can be obtained as a projection of a vertex (8) onto the two-body symmetric subspace (cf. Appendix A). Interestingly, it can be parametrized by the populations $\xi_{p,i}$ with $p = 1,\dots,k$ and $i = 1,\dots,n_p$, representing the number of p-partite subgroups $\mathcal{A}_l$ in the k partition of the set $\{A_1,\dots,A_N\}$ (cf. Sec. II B) that are adopting the same "strategy" from the list $\{\vec{S}(p,i)\}_{p,i}$. Indeed, since we are addressing permutationally invariant quantities, these are insensitive to the assignment of a strategy to a specific group of parties; hence, the only relevant information is about the number of parties adopting each given set of correlations [22,25].

Recall that parties are divided into subsets of size at most k, and each subset of size p chooses one out of n_p strategies. Therefore, the populations $\xi_{p,i}$, weighted by p, form a partition of N; that is, $\xi_{p,i}$ are integer numbers satisfying the conditions $\xi_{p,i} \geqslant 0$ and

$$\sum_{p=1}^{k}\sum_{i=1}^{n_p} p\,\xi_{p,i} = N. \tag{14}$$

By running over all populations $\xi_{p,i}$ obeying (14), one spans the whole set of vertices of the polytope $\mathcal{P}_{N,k}^{2,S}$. Moreover, denoting by $\vec{\xi}$ the vector with components $\xi_{p,i}$, the symmetrized one- and two-body expectation values for the vertices of $\mathcal{P}_{N,k}^{2,S}$ can be expressed as

$$S_x(\vec{\xi}) = \sum_{p=1}^{k}\sum_{i=1}^{n_p} \xi_{p,i} S_x(p,i) \tag{15}$$

and

$$\begin{aligned} S_{xy}(\vec{\xi}) = &\sum_{p=1}^{k}\sum_{i=1}^{n_p} \xi_{p,i} S_{xy}(p,i) \\ &+ \sum_{p=1}^{k}\sum_{i=1}^{n_p} \xi_{p,i}(\xi_{p,i}-1) S_x(p,i) S_y(p,i) \\ &+ \sum_{\{p,i\}\neq\{q,j\}} \xi_{p,i}\xi_{q,j} S_x(p,i) S_y(q,j), \end{aligned} \tag{16}$$

where we used the fact that $\langle M_x^{(i)} M_y^{(j)}\rangle = \langle M_x^{(i)}\rangle\langle M_y^{(j)}\rangle$ whenever the parties i and j belong to different groups, and $\{p,i\} \neq \{q,j\}$ means that $p \neq q$ or $i \neq j$ (cf. Appendix B for the details of the calculation and Fig. 1 for a pictorial representation).

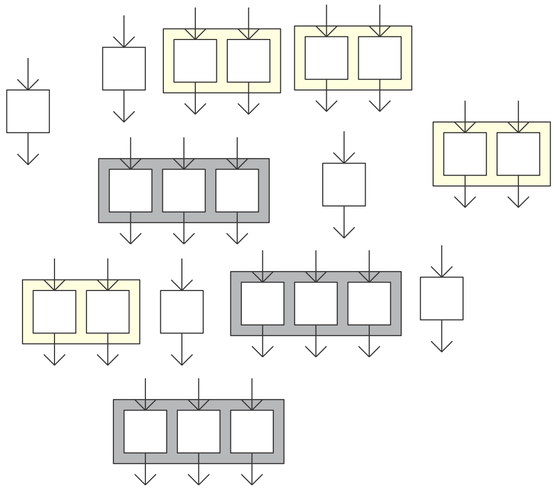

FIG. 1. A possible L_k partition corresponding to a vertex of $\mathcal{P}^{2,S}_{N,k}$, for $N = 22$, $k = 3$, and $L = 12$. Here, we have taken a 12_3 partition consisting of five subsets of size 1, four subsets of size 2, and three subsets of size 3. Each of the five parties that are alone can choose one out of the $n_1 = 4$ possible local deterministic strategies. Counting how many particles choose the ith strategy, where $1 \leqslant i \leqslant n_1$, determines $\xi_{1,i}$. Each pair of particles highlighted in yellow can choose one out of the n_2 possible Popescu-Rohrlich (PR) boxes of $\mathcal{NS}_2$ and each triplet of particles highlighted in gray can choose one out of the n_3 PR boxes highlighted in gray. The remaining coordinates of $\vec{\xi}$ are obtained analogously by counting. In Fig. 6, a detailed explanation is given, showing how to obtain the values (15) and (B9) from $\vec{\xi}$.

Hence, from (15) and (16) we see that all the vertices of the $\mathcal{P}^{2,S}_{N,k}$ can be directly computed as a function of the vertices of the projected no-signaling polytopes. In particular, their number is entirely encoded in the population vector $\vec{\xi}$ and grows only as $O(N^k)$ (see Appendix C for a proof of the scaling).

Therefore, given that the expressions above allow us to compute efficiently the vertices of $\mathcal{P}^{2,S}_{N,k}$, the only remaining difficulty is to obtain the lists $\{\vec{S}(p,i)\}_{p,i}$ of vertices of the projected no-signaling polytopes, which we address in Sec. IV B.

B. Projecting the nonsignaling polytopes

In order to generate the vertices of the symmetric two-body polytope of k-producible correlations $\mathcal{P}^{2,S}_{N,k}$, we need to know the vertices of the nonsignaling polytope $\mathcal{NS}_p$ in the two-body symmetric space for $2 \leqslant p \leqslant k$ parties. To this aim, we need to determine its projection $\mathcal{NS}^{2,S}_p$ onto the two-body symmetric space spanned by (10) for any $p = 2, \ldots, k$.

As already mentioned, the vertices of $\mathcal{NS}_p$ for $p > 3$ are unknown and difficult to determine. In contrast, its facets are easy to describe by the positivity constraints, which in the correlator picture can be stated as [cf. Eq. (5)]

$$\sum_{k=1}^{p} \sum_{1\leqslant i_1<\ldots<i_k\leqslant p} a_{i_1}\ldots a_{i_k}\big\langle M^{(i_1)}_{x_{i_1}}\ldots M^{(i_k)}_{x_{i_k}}\big\rangle + 1 \geqslant 0, \tag{17}$$

for all the possible outcomes $a_{i_1}, \ldots, a_{i_N} = \pm 1$ and measurement choices $x_1, \ldots, x_N = 0, 1$.

Recall that the default approach to find the projections $\mathcal{NS}^{2,S}_p$ onto the two-body symmetric space, namely the Fourier-Motzkin procedure (see Appendix A), becomes impractical already for $p = 3$, due to exponential number of components to project out. Nevertheless, in what follows we will show how to overcome this difficulty by making use of the properties of the $\mathcal{NS}_p$ set with respect to the projection we are interested to perform.

To this end, let us denote by V_2 the subspace spanned by one- and two-body expectation values (9) and by V_{sym} the subspace spanned by the symmetrized correlators of any order:

$$S_{x_1\ldots x_l} = \sum_{i_1\neq\ldots\neq i_l=1}^{k} \big\langle M^{(i_1)}_{x_1}\ldots M^{(i_l)}_{x_l}\big\rangle \tag{18}$$

with $x_i = 0, 1$ and $l = 1, \ldots, p$. We then define π_2, π_{sym} as the linear projections onto the V_2 and V_{sym} respectively; that is, π_2 discards all correlators that involve more than two parties and π_{sym} sums all the permutations of the correlators of a given order. We will use the fact that, in this notation, the projection we want to compute can be divided into two intermediate steps as $P = \pi_2 \circ \pi_{\text{sym}} = \pi_{\text{sym}} \circ \pi_2$, where the order in which the projections π_2 and π_{sym} are applied to $\mathcal{NS}_p$ does not change the result. In other words, the following diagram is commutative:

$$\begin{array}{ccc} \mathcal{NS}_p & \xrightarrow{\pi_2} & \mathcal{NS}^2_p \\ \big\downarrow \pi_{\text{sym}} & & \big\downarrow \pi_{\text{sym}} \\ \mathcal{NS}^S_p & \xrightarrow{\pi_2} & \mathcal{NS}^{2,S}_p \end{array}.$$

This property follows from the fact that each coordinate of $\mathcal{NS}_p$ participates solely in one coordinate of $\mathcal{NS}^{2,S}_p$ [cf. Eq. (10)].

We therefore choose to perform the projection as $P = \pi_2 \circ \pi_{\text{sym}}$, hence first computing the symmetrize polytope $\mathcal{NS}^S_p$ and then projecting it onto the two-body space. At this stage, it is crucial to note that the no-signaling set is invariant under the parties' permutation. We now prove that this implies a very useful result, namely that the projection of this set onto V_{sym} coincides with the intersection between $\mathcal{NS}_p$ and V_{sym}, an idea which we illustrate in Fig. 2, i.e.,

$$\text{int}_{\text{sym}}(\mathcal{NS}_p) = \pi_{\text{sym}}(\mathcal{NS}_p). \tag{19}$$

Let us first explain what we mean by the intersection. To do so, consider the coordinates

$$T^{j_1\ldots j_l}_{x_1\ldots x_l} = \left(\sum_{i_1\neq\ldots\neq i_l=1}^{k}\right)\big\langle M^{(j_1)}_{x_1}\ldots M^{(j_l)}_{x_l}\big\rangle - S_{x_1\ldots x_l}. \tag{20}$$

Taken together with the symmetrized S of Eq. (18), these correlators provide an overcomplete parametrization of the no-signaling probability space: Any correlator $\langle M^{(j_1)}_{x_1}\ldots M^{(j_l)}_{x_l}\rangle$ can be recovered from the corresponding T and S variables. Moreover, these coordinates conveniently identify the subspaces that we are interested in: The symmetric subspace is spanned by the S variables, while its orthogonal complement is spanned by the T variables. In other

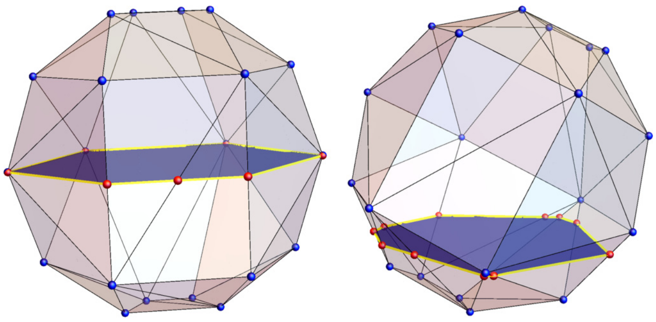

FIG. 2. A cartoon picture illustrating the cases when projection and intersection of a polytope with a hyperplane are the same operation (left) and the generic case in which the intersection of a polytope with a hyperplane is strictly contained into its projection onto the same hyperplane (right).

words, all correlations in the symmetric subspace have all T components equal to zero (however, the variables themselves before projection need not be zero). Moreover, the one- and two-body space has all S and T parameters equal to 0 for $l > 2$.

Using the above notation, we define $\mathrm{int}_{\mathrm{sym}}(\mathcal{NS}_p)$ as the set that contains all no-signaling correlations for which all the variables $T^{j_1\ldots j_l}_{x_1\ldots x_l} = 0$ (cf. Appendix A for a more formal introduction to projection and intersection). Now, if a vertex v of $\mathcal{NS}_p$ (which may have both nonzero S and T components) leads to an extremal vertex after projection onto V_{sym}, then all images $v_\alpha = \tau_\alpha(v)$ of v under the party permutations $\{\tau_\alpha\}_\alpha$ are also in $\mathcal{NS}_p$ and lead to the same point in V_{sym} after projection. This follows directly from the invariance of $\mathcal{NS}_p$ under party permutations. Then, the convex combination of these points $\overline{v} \propto \sum_\alpha v_\alpha$ also gives rise to the same extremal point in V_{sym}. However, a direct computation shows that the point $\overline{v}$ already belongs to the symmetric subspace, because all of its T variables are zero. Hence, all extremal points of the projection of $\mathcal{NS}_p$ onto the symmetric subspace belong to the intersection of the no-signaling polytope with the symmetric subspace, and we can replace the projection operation π_{sym} by the intersection.

The main advantage of this approach is that the facets of the intersection of a polytope can be efficiently computed from the facets of the original one. Therefore, we only need to apply the Fourier-Motzkin method to perform the projection of $\mathcal{NS}^S_p$ onto the two-body space V_2. In this case, the number of variables to discard does not grow exponentially with N. Indeed, the number of symmetric correlators $S_{x_1\ldots x_l}$ with $x_j = 0, 1$ and $l = 1, \ldots, p$ scales as $(1/2)(p+1)(p+2) - 1$ and, since one has to discard all the terms with $l > 2$, we need to eliminate only $(1/2)(p+1)(p+2) - 6 \approx O(p^2)$ terms.

This simplification allows us to obtain the complete list of vertices of the $\mathcal{NS}^{2,S}_N$ polytopes for $N \leqslant 6$ particles, thus improving significantly the already known results. For the $N = 2, 3, 4$ cases, the lists of vertices are presented in Tables I–III in Appendix D, whereas in the case $N = 5, 6$ the list contains more than a hundred vertices and therefore we could not present it here. In the next section, we implement these findings to construct Bell-like inequalities detecting k-nonlocality in multipartite correlations.

V. BELL-LIKE INEQUALITIES FOR NONLOCALITY DEPTH FROM TWO-BODY CORRELATIONS

We are now ready to demonstrate that two-body Bell-like inequalities are capable of witnessing nonlocality depth in multipartite correlations. First of all, we remind readers that, by following the procedure given in Sec. IV A, we are able to construct the list of vertices of the k-nonlocal two-body symmetric polytopes for any number of parties N and producibility $k \leqslant 6$. By solving the convex hull problem, such lists allow us to derive the corresponding complete set of facets of the k-nonlocal polytopes. This can be done via the dual description method, which is implemented in such software as CDD [48], and, thanks to both the low dimension of the space and the polynomial scaling of the k-producible vertices, we are able to do so for scenarios involving up to $N = 15$ parties.

In particular, since these inequalities can test against k-producibility with $k \leqslant 6$, we can identify all the symmetric two-body inequalities that detect genuine multipartite nonlocality (GMNL) for systems of $N \leqslant 7$ particles (see Appendix E for the complete lists). Interestingly, we find that no inequality of such kind can be violated by quantum mechanics in the tripartite case. That is, symmetric two-body correlations do not provide enough information to detect GMNL in three-partite quantum states. This is no longer the case for four parties; indeed, the facet

$$\mathcal{I}^4_{\mathrm{GMNL}} := -12S_0 + 9S_1 + 3S_{00} - 6S_{01} + \tfrac{1}{2}S_{11} + 42 \geqslant 0 \tag{21}$$

detects GMNL and is violated by quantum mechanics with a ratio $(\beta_Q - \beta_3)/\beta_3$ of at least 1.3%, where β_Q is the maximal quantum value of I^4_{GMNL} and $\beta_3 = 42$ is the bound for nonlocality depth 3.

Interestingly, our lists of inequalities sometimes contain also the Bell expressions introduced already in Refs. [22,25], thus showing that such classes are actually capable of detecting a nonlocality depth higher than 2. In particular, we can find inequalities that test against any k-producibility for $k \leqslant 5$ that belong to the class (91) introduced in Ref. [25]. This class is particulary interesting since it was shown to be violated by Dicke states. Moreover, among the facets of the GMNL polytope for $N = 5$, we find the following inequality:

$$\mathcal{I}_W = 28S_0 + 28S_1 + 2S_{00} + 9S_{01} + 2S_{11} + 116 \geqslant 0, \tag{22}$$

which has a very similar structure to class (91) of Ref. [25]. Indeed, it can be shown that it is possible to violate such inequality with the five-partite Dicke state with one excitation, also known as the W state. Lastly, we notice that the Bell expression (6) from Ref. [22], which for the sake of completeness we state here as

$$\mathcal{I} := 2S_0 + \tfrac{1}{2}S_{00} + S_{01} + \tfrac{1}{2}S_{11}, \tag{23}$$

appears in our lists sometimes as well, with a classical bound that clearly depends on degree of nonlocality depth that one is interested in detecting. This is a particularly useful feature, since it implies that by the use of a single inequality one can infer the nonlocality depth by the amount of the quantum violation that is observed. Because of this property and also its relevance for experimental implementation (see

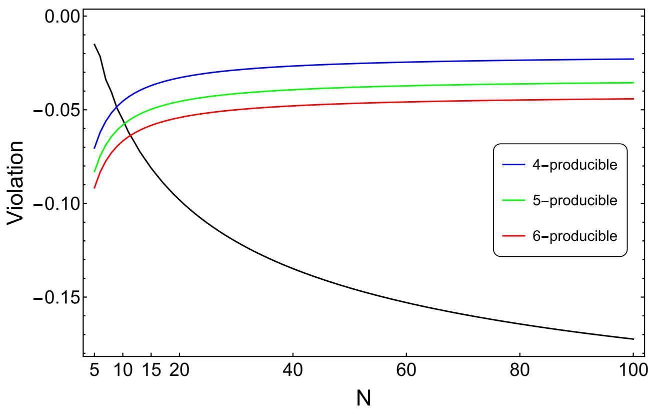

FIG. 3. Plot of the quantum violation $(\beta_Q - \beta_1)/2N$ (black line) of the inequality (23) obtainable by following the procedure in Ref. [25]. The violation is compared with the—appropriately rescaled—k-producible bounds $(\beta_k - \beta_1)/2N$ for the same inequality (colored lines) for values $k = 4, 5, 6$ (curves shown from top to bottom). Recall that the bounds for $k \leqslant 3$ coincide with the local one, and hence they are not shown in the plot.

Refs. [23,30]), we focus on this last inequality and determine its β_k for $k = 2, \ldots, 6$ and any number of parties (see Appendix F for the details of the calculations). In particular, we first obtain that for the simples cases of $k = 2, 3$, the k-producible bound coincides with the local, i.e., $\beta_k = 2N$, meaning that the violation of such inequality actually detects already a nonlocality depth of at least 4. Then, for the higher values of k, we are able show that the bound takes the following simple form:

$$\beta_k = 2N + \tfrac{1}{2} + \alpha_k N, \tag{24}$$

where the parameter α_k encodes the dependence on the nonlocality depth. More explicitly, we obtain $\alpha_4 = 2/49$, $\alpha_5 = 8/121$, and $\alpha_6 = 1/12$. After having introduced k-producible bounds for inequality (23), it is important to show that they can be used in practice to witness the nonlocality depth that could be displayed by quantum states. First of all, we have to show that the different bounds β_k can be violated by correlations obtained by properly choosing a quantum state and some local measurements. This can be done in a scalable way by following the procedure in Ref. [25] and constructing the permutationally invariant Bell operator corresponding to the expression (23). Notice that to do so we assume for simplicity that each party performs the same measurements:

$$\begin{aligned} M_0^{(i)} &= \cos(\theta)\sigma_z^{(i)} + \sin(\theta)\sigma_x^{(i)}, \\ M_1^{(i)} &= \cos(\phi)\sigma_z^{(i)} + \sin(\phi)\sigma_x^{(i)}, \end{aligned} \tag{25}$$

where $\theta, \phi \in [0, 2\pi)$, and σ_z and σ_x are the standard Pauli matrices. Then, by computing the minimal eigenvalue of the resulting Bell operator $\mathcal{B}(\theta, \phi)$ and optimizing over the choice of angles, one obtains the maximal quantum violation of (23) attainable with same measurements settings on each site. By performing these numerical checks, whose results are compared in Fig. 3, it is possible to show that the bound β_k for $k \leqslant 3$ starts being violated for $N = 5$ parties, while for the higher cases $k = 4, 5$ the violation appears from $N = 9$ and $N = 11$ respectively. Moreover, if we take into account the analytical class of states introduced in Ref. [25] (cf. Sec. V B), we can show that for a sufficiently high number of parties it violates all the bounds that we have just derived. Indeed, let us recall that this class of states can achieve a relative violation $(\beta_Q - \beta_1)/\beta_1$ of (23) that tends to $-1/4$ when $N \to \infty$. By using this result, it is easy to show that β_Q exceeds β_k for any $k \leqslant 6$, at least in the asymptotic limit, confirming the numerical evidence shown in Fig. 3. To conclude, in the following section we also present how to apply our results to an experimental setting.

VI. EXPERIMENTAL WITNESSING OF k-BODY BELL CORRELATIONS

The inequalities introduced in the previous sections provide efficient tools to study the nonlocality depth of correlations produced by multipartite states. In fact, being based on two-body correlations only, they require at most performing $O(N^2)$ measurements. This makes these inequalities particularly amenable for currently available photonic and atomic systems composed of few tens of particles [49–51].

Moreover, as already noticed in Refs. [22,23,27], the symmetrized one- and two-body correlators (10) can be estimated by means of collective measurements. Recall, however, that this is possible only when the measurements performed locally correspond to spin projections along well-defined directions. Under this additional assumption, inequalities of the form (11) thus give rise to device-dependent witnesses that quantify the amount of Bell correlations exhibited by a many-body system. More precisely, violating such witnesses detects *Bell correlations depth* in the state: Violation of Bell correlation witnesses for depth k certifies the presence of an entangled state that could display nonlocal correlations of depth $k + 1$ if the single particles were brought far apart from each other and addressed separately.

In the following subsections, we study in more detail the available methods to quantify Bell correlation depths in a many-body state. First of all, we derive the witness corresponding to already known full-body inequalities capable of detecting nonlocality depth, such as the Mermin and Svetlichny Bell inequalities. Interestingly, we show that such a witness can actually be estimated by collective spin measurements along two directions only, although requiring a parity measurement that is very demanding for large systems. This shows how the two-body Bell inequalities introduced in this work can provide a real advantage in terms of experimental feasibility. We demonstrate this advantage by deriving a witness associated to inequality (23) and, by making use of already available data, show how it can be applied to detect Bell correlations depth in a BEC composed of hundreds of particles.

A. Witnessing genuine nonlocality from Svetlichny and Mermin inequalities

The Mermin and Svetlichny Bell expressions are known to be suitable for the detection of nonlocality depth in multipartite systems [33]. They thus suit our investigations very well. We here show the form of the corresponding witnesses for nonlocality depth. Let us begin with the Svetlichny Bell expressions written in the following form [52]:

$$I_N^{\rm Svet} = 2^{-N/2}\left[\sum_{\mathbf{x}|\mathbf{s}=0 \pmod 2} (-1)^{\mathbf{s}/2} E_{\mathbf{x}} + \sum_{\mathbf{x}|\mathbf{s}=1 \pmod 2} (-1)^{(\mathbf{s}-1)/2} E_{\mathbf{x}}\right], \tag{26}$$

where $\mathbf{s} = \sum_i x_i$ is the sum of all parties' settings (recall that $x_i \in \{0, 1\}$), $\mathbf{x}|\mathbf{s} = i \pmod 2$ means that the summation is over those $\mathbf{x}$'s for which $\mathbf{s}$ is even for $i = 0$ or odd for $i = 1$, and, finally,

$$E_{\mathbf{x}} = \langle M_{x_1}^{(1)} \dots M_{x_N}^{(N)} \rangle \tag{27}$$

is a short-hand notation for an N-partite correlator. Using the same notation, we also introduce the Mermin Bell expression [53], namely

$$I_N^{\rm Mermin} = 2^{-(N-1)/2}\left[\sum_{\mathbf{x}|\mathbf{s}=0 \pmod 2} (-1)^{\mathbf{s}/2} E_{\mathbf{x}}\right]. \tag{28}$$

For both the above inequalities, the k-producible bounds β_k can be explicitly computed and they can be used to reveal different nonlocality depth from observed correlations (cf. Appendix G for more details). In particular, the $(N-1)$-nonlocal bound is always smaller than the maximal quantum violation β_Q, meaning that these inequalities can detect genuine multipartite nonlocality for any number of particles. However, the sums in Eqs. (26) and (28) involve 2^N terms in total, making the Svetlichny and Mermin inequalities very difficult to test in systems with a large number of parties. Nevertheless, in the following we will show that if one is willing to assume that the measurements are well calibrated spin projections, then one can derive a witness that involves only collective measurement in two directions.

First of all, let us construct Bell operators for the Bell expressions (26) and (28). For this, we recall that the measurement settings maximizing the quantum value of the Svetlichny inequality, for a $|{\rm GHZ}_N^{\pm}\rangle$ state, $|{\rm GHZ}_{\rm N}^{\pm}\rangle = (|0\rangle^{\otimes {\rm N}} \pm |1\rangle^{\otimes {\rm N}})/\sqrt{2}$, are

$$M_j^{(i)} = \cos(\phi_j)\,\sigma_x + \sin(\phi_j)\,\sigma_y\,, \quad \phi_j = -\frac{\pi}{4N} + j\frac{\pi}{2}, \tag{29}$$

with $j \in 0, 1$. Similarly, the Mermin inequality is maximally violated by the same $|{\rm GHZ}_N^{+}\rangle$ state when the measurements are $M_0^{(i)} = \sigma_x$ and $M_1^{(i)} = \sigma_y$ for each party $i = 1, \dots, N$. By substituting these settings in their respective inequalities, we find that both the Svetlichny and Mermin operators take the following very simple form:

$$\mathcal{B}_N^{\rm Svetlichny} = \mathcal{B}_N^{\rm Mermin} = \mathcal{B}_N = 2^{(N-1)/2}(|0\rangle\langle 1|^{\otimes N} + |1\rangle\langle 0|^{\otimes N}). \tag{30}$$

We can thus derive a common witness with which the nonlocality depth of any multipartite system can be evaluated. In particular, one can prove that the above operator can be bounded in the following way:

$$\mathcal{B}_N = \sqrt{2}^{N-1}(|{\rm GHZ}_N^{+}\rangle\langle{\rm GHZ}_N^{+}| - |{\rm GHZ}_N^{-}\rangle\langle{\rm GHZ}_N^{-}|) \geqslant \sqrt{2}^{N-1}\left[\sigma_x^1 \dots \sigma_x^N + 4J_{\mathbf{z}}^2 - N^2\mathbb{1}\right], \tag{31}$$

where $J_{\mathbf{n}} = (1/2)\sum_{i=1}^N \boldsymbol{\sigma}^{(i)} \cdot \mathbf{n}$ is the collective spin operator along the direction $\mathbf{n}$. Combining the k-nonlocal bounds of the Svetlichny and Mermin Bell expressions given in Appendix G then allows us to write the following witness of Bell correlations depth:

$$\langle \mathcal{B}_N \rangle = \sqrt{2}^{N-1}\langle \sigma_x^1 \dots \sigma_x^N + 4J_{\mathbf{z}}^2 - N^2\mathbb{1}\rangle \leqslant 2^{(N-\lceil \frac{N}{k} \rceil)/2}. \tag{32}$$

Inequality (32) shows that two settings are enough to conclude about the Bell correlation depth of a given state, that is, to test the capability of a state to violate a Svetlichny or Mermin bound for k-nonlocality. This provides a way to detect various depths of Bell correlations with just two measurement settings and no individual addressing of the parties. In particular, since the GHZ state saturates all the inequalities we used in this section, the operator $\mathcal{B}_N$ is able to detect that GHZ states are genuinely Bell correlated.

Still, this scheme involves one parity measurement: the N-body term in the x direction. It is worth noticing that the evaluation of this term does not require an estimation of all the moment of the spin operator $J_{\mathbf{x}}$ in the x direction (which would require a gigantic amount of statistics to be evaluated properly whenever $N \gg 1$). Rather, this term corresponds to the parity of the spin operator $J_{\mathbf{x}}$, i.e., a binary quantity, and can thus be evaluated efficiently. However, an extreme resolution is required to estimate this quantity; failure to distinguish between two successive values of $J_{\mathbf{x}}$ can entirely randomize its parity.

The next section aims at detecting the Bell correlation depth of multipartite states with two-body correlators only.

B. Witnessing with two-body correlations only

In the same spirit as Refs. [22,23,27], we derive a witness for Bell correlations of depth k from the expression $\mathcal{I} + \beta_k \geqslant 0$, where $\mathcal{I}$ is defined in Eq. (23). We assume that $M_0^{(i)}$ and $M_1^{(i)}$ are spin projection measurements on the ith party, along directions $\mathbf{n}$ and $\mathbf{m}$, respectively. This allows us to write $M_0^{(i)} = \boldsymbol{\sigma}^{(i)} \cdot \mathbf{n}$ and $M_1^{(i)} = \boldsymbol{\sigma}^{(i)} \cdot \mathbf{m}$, where $\boldsymbol{\sigma}^{(i)}$ is the vector of Pauli matrices acting on the ith party, and to express all correlators appearing in the Bell inequality as measurements of the collective spin operator $J_{\mathbf{n}}$. With the substitution $\mathbf{m} = 2(\mathbf{a}\cdot\mathbf{n})\mathbf{a} - \mathbf{n}$, we arrive at the inequality (see Ref. [23] for details)

$$-\left|\left\langle \frac{J_{\mathbf{n}}}{N/2} \right\rangle\right| + (\mathbf{a}\cdot\mathbf{n})^2\left\langle \frac{J_{\mathbf{a}}^2}{N/4} \right\rangle - (\mathbf{a}\cdot\mathbf{n})^2 + \frac{\beta_k}{2N} \geqslant 0, \tag{33}$$

which is satisfied by all states with Bell correlations of depth at most k. In other words, the violation of Ineq. (33) witnesses that the state of the system contains Bell correlations of depth (at least) $(k+1)$.

It is now convenient to define the spin contrast $\mathcal{C}_{\mathbf{n}} = \langle 2J_{\mathbf{n}}/N\rangle$ and the scaled second moment $\zeta_{\mathbf{a}}^2 = \langle 4J_{\mathbf{a}}^2/N\rangle$. Furthermore, we express $\mathbf{n} = \mathbf{a}\cos(\theta) + \mathbf{b}\sin(\theta)\cos(\phi) + \mathbf{c}\sin(\theta)\sin(\phi)$, with the orthonormal vectors $\mathbf{a}$, $\mathbf{b}$, and $\mathbf{c} = \mathbf{a}\times\mathbf{b}$ with $\times$ denoting the vector product. With these

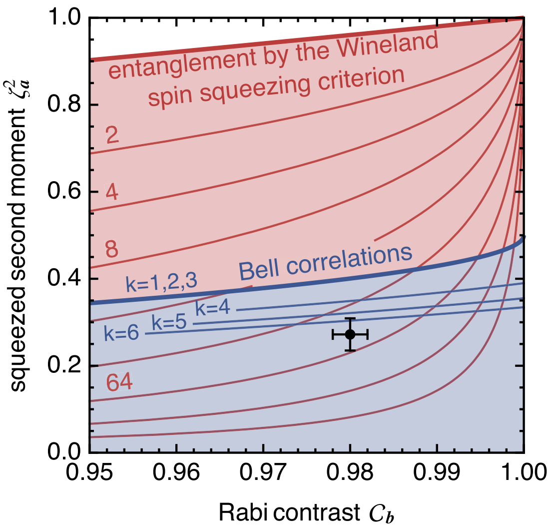

FIG. 4. Quantification of the Bell correlation depth in a BEC with inequality (34) and connection to spin squeezing and entanglement. Black: the data reported in Ref. [23] expressed in terms of the Rabi contrast $\mathcal{C}_{\mathbf{b}}$ and the squeezed second moment $\zeta_{\mathbf{a}}^2$, with 1σ error bars. The number of particles is $N = 480$. Blue shaded region: Bell correlations detected by violation of inequality (34) for $k = 1$. Red shaded region: entanglement witnessed by spin squeezing [54,56]. Red lines: limits on $\zeta_{\mathbf{a}}^2$ below which there is at least $(k+1)$-particle entanglement [55], increasing in powers of 2 up to $k = 256$. Blue lines: limits on $\zeta_{\mathbf{a}}^2$ below which there are Bell correlations of depth at least $k+1$, for $k = 1, \ldots, 6$.

definitions, one can obtain the witness [23]

$$\zeta_{\mathbf{a}}^2 \geqslant \frac{2 - \beta_k/(2N) - \sqrt{[\beta_k/(2N)]^2 - \mathcal{C}_{\mathbf{b}}^2}}{2}, \tag{34}$$

which involves the measurements of $\zeta_{\mathbf{a}}$ and $\mathcal{C}_{\mathbf{b}}$, for the two orthogonal directions **a** and **b**. The violation of Ineq. (34), for a given β_k, witnesses that the state contains Bell correlations with a depth of (at least) $k+1$.

An interesting comparison is made with the Wineland spin-squeezing criterion [54], according to which entanglement is present if $\zeta_{\mathbf{a}}^2 < \mathcal{C}_{\mathbf{b}}^2$ [23]. This criterion was also shown to be able to quantify the degree of entanglement in the state [55], and $(k+1)$-particle entanglement is witnessed by measuring values of $\zeta_{\mathbf{a}}^2$ below some threshold; see Fig. 4 (red lines). In Fig. 4, we plot the bounds given by Eq. (34), for $k = 1, \ldots, 6$, together with the entanglement bound obtained from the Wineland criterion [55] and the experimental point measured in Ref. [23]. A statistical analysis on the probability distribution estimated experimentally [23] gives likelihoods of 99.9%, 97.5%, 90.3%, and 80.8% for 1/2/3-, 4-, 5-, and 6-body nonlocality respectively. This likelihood can be interpreted as, for example, a p value of $1 - 80.8\% = 19.2\%$ for rejecting the following hypothesis: The experimental data were generated by a state that has no 6-body nonlocality, in the presence of Gaussian noise.

VII. CONCLUSION

We study the problem of finding efficient ways to detect the nonlocality depth of quantum correlations. Nonlocality depth is a relevant concept in the study of multipartite systems, because it contains the information of how many particles share genuine Bell correlations in their state. In analogy to the case of nonlocality, detecting nonlocality depth is a computationally very demanding problem.

We first exploit the framework of two-body symmetric correlations introduced in Ref. [22] to provide means of certifying nonlocality depth in many-body physics that meet the requirements of current experiments. By developing a general framework to describe the set of correlations of a given nonlocality depth, we are able to show that two-body symmetric correlations are enough to distinguish such depth for $k \leqslant 6$. We do so by completely characterizing the set of Bell inequalities that detect k-nonlocality with respect to nonsignaling resources for values of $k \leqslant 6$ and a fixed number of particle $N \leqslant 15$. Remarkably, we also show that detecting nonlocality depth can be done efficiently for any fixed k, that is, involving a polynomial amount of computational resources. Moreover, we take an explicit example of inequality and show that it can be used to witness the depth of Bell correlations for $k \leqslant 6$ and any number of parties.

Lastly, we comment on the practical application of our techniques to large many-body states. As an initial comparison, we turn to the known Bell inequalities of Mermin and Svetlichny that allow for detection of nonlocality depth in multipartite quantum states. We show that if the measurements are trusted, such inequalities can be used to derive witnesses that can reveal genuine Bell correlations with two collective measurements in systems where many-body correlation functions can be evaluated. This approach based on two-body correlations is advantageous because it does not utilize the parity measurement which is extremely challenging to perform in large systems. We therefore show that the witnesses that can be derived from our two-body Bell inequality can be successfully applied to already available experimental data from a Bose-Einstein condensate. We stress that such a witness should be considered as a tool for many-body states that allows us to quantify correlations that are stronger than entanglement. In particular, we proposed the notion of entangled state displaying Bell correlation depth, that is, a many-body state that, if the particles were brought apart, would be capable of producing correlations with a nonocality depth k.

Our results pave the way for a more refined study of Bell correlations in many-body systems by presenting available techniques to determine the amount of particles sharing Bell correlations in these systems. As a future direction to investigate, it would be interesting to derive inequalities that test for higher nonlocality depth than 6, as it is already possible to do in the case of entanglement. In particular, a more ambitious direction would be to find ways to assess genuine Bell correlations in systems of hundreds of particles without relying on parity measurements. This would give a convenient way to prove that all the particles in the system are genuinely sharing Bell correlations.

As argued in the previous sections, the main challenge for these purposes consists in characterizing the no-signaling set of multipartite correlations in the subspace of two-body permutationally invariant correlators. We are able to do so only for the cases of low number of parties, while a general and efficient method is still missing. Therefore, a more technical but still interesting question would be to find such a general characterization.

Another possible research direction would be to consider inequalities involving more than two settings per party. The resulting witness could still only involve two measurement directions and provide improved bounds. In particular, it would be interesting to find the k-nonlocality bounds for the family of inequalities in Ref. [27] admitting an arbitrary number of settings.

It would also be interesting to design witnesses suited for specific families of states other than the GHZ state such as all the graph states or the Dicke states.

Except for the witnesses we derived from the Svetlichny inequalities, the witnesses we obtained here rely on the notion of Svetlichny models defined in terms of no-signaling resources. It would be interesting to see if the bounds derived here remain valid with respect to the sequential and signaling models, in which case they could also demonstrate this stronger form of k-nonlocality. Otherwise, it would be interesting to find other two-body inequalities suited for this task.

Lastly, we stress that our results can already be applied to experimentally detect in a Bell test genuine multipartite nonlocality for systems of size up to $N = 7$. In particular, since the inequalities that we introduce consist only of two-body correlators, such detection would require only an $O(N^2)$ amount of measurements, contrarily to already known inequalities, such as Mermin's, that involve measuring an exponential amount of correlators.

ACKNOWLEDGMENTS

We acknowledge support from the Spanish MINECO (SEVERO OCHOA Grant No. SEV-2015-0522, FISICATEAMO Grant No. FIS2016-79508-P, QIBEQI Grant No. FIS2016-80773-P, and a SEVEREO OCHOA Ph.D. fellowship), ERC AdG OSYRIS (ERC-2013-ADG Grant No. 339106) and CoG QITBOX (ERC-2013-COG Grant No. 617337), the AXA Chair in Quantum Information Science, Generalitat de Catalunya (Grant No. 2014-SGR-874, Grant No. 2014-SGR-875, and CERCA Program), EU FET-PRO QUIC and Fundacio Privada Cellex, the Swiss National Science Foundation (SNSF) through the NCCR QIST and Grant No. PP00P2-150579, and the Army Research Laboratory Center for Distributed Quantum Information via the project SciNet. This project has received funding from the European Union's Horizon 2020 research and innovation programme under the Marie Skłodowska-Curie Grant Agreements No. 748549 and No. 705109. R.A. acknowledges the support from the Foundation for Polish Science through the First TEAM project (First TEAM/2017-4/31) cofinanced by the European Union under the European Regional Development Fund. J.T. acknowledges support from the Alexander von Humboldt Foundation. M.F. was supported by the Swiss National Science Foundation through Grant No. 200020_169591.

APPENDIX A: POLYTOPES

Here, we provide the definitions of polytopes and their duals. We then show how to project a polytope P onto a given subspace V as well as how to intersect P and V.

A convex polytope, in what follows we call simply "polytope," is a subset in a linear space $\mathbb{R}^d$ with some finite d defined as the convex hull of a finite number of points $\vec{e}_i \in \mathbb{R}^d$ $(i = 1, \dots, K)$, i.e.,

$$P = \left\{ \vec{p} \in \mathbb{R}^d \mid \vec{p} = \sum_{i=1}^{m} q_i \vec{e}_i \right. \\ \left. \text{such that } q_i \geqslant 0 \text{ and } \sum_{i=1}^{m} q_i = 1 \right\}. \tag{A1}$$

Here $\vec{e}_i$ are the vertices of P. Alternatively, one can define a polytope to be an intersection of a finite number of half-spaces, meaning that P is described by a finite set of inequalities:

$$P = \{\vec{p} \in \mathbb{R}^d \mid \vec{f}_i \cdot \vec{p} \leqslant \beta_i \text{ with } \vec{f}_i \in \mathbb{R}^d \text{ and } \beta_i \in \mathbb{R}\}. \tag{A2}$$

Facets of a polytope P are its intersections with the hyperplanes $\vec{f}_i \cdot \vec{p} = \beta_i$. Let us also define the dual of a polytope P to be

$$P^* = \{\vec{f} \in \mathbb{R}^d \mid \vec{f} \cdot \vec{p} \geqslant 0 \text{ for all } \vec{p} \in P\}. \tag{A3}$$

For our convenience, in Eqs. (A2) and (A3), we use different conventions regarding inequalities when defining a polytope and its dual. However, it should be noticed that it is not difficult to transform inequalities appearing in Eq. (A2) into those in Eq. (A3) and vice versa: In particular, to obtain inequalities in (A3) from those in (A2), it suffices to incorporate the free parameter β_i and the sign into the vector $\vec{f}$, in the first case exploiting the fact that for a given choice of measurements, elements of the vector $\vec{p}$ are normalized.

Let us now discuss projections of polytopes. Consider a subspace $V \subset \mathbb{R}^d$ and denote by $\pi_V : \mathbb{R}^d \to V$ the projection onto it. Imagine then that we want to project a given polytope $P \subset \mathbb{R}^d$ onto V. There are two ways of determining the action of π_V on P. First, $\pi_V(P)$ can be straightforwardly defined in terms of projection of its vertices, i.e.,

$$\pi_V(P) = \left\{ \vec{p} \in V \mid \vec{p} = \sum_{i=1}^{K} q_i \pi_V(\vec{e}_i) \right. \\ \left. \text{such that } q_i \geqslant 0 \text{ and } \sum_{i} q_i = 1 \right\}. \tag{A4}$$

Notice that the projections of the vertices $\vec{e}_i$, $\pi_V(\vec{e}_i)$ might not be vertices of the projected polytope $\pi_V(P)$. On the other hand, a vertex of $\pi_V(P)$ must come from a vertex of P under the projection π_V.

However, in certain situations it is much easier to describe a polytope by using inequalities instead of vertices. In fact, there are polytopes such as those formed by correlations fulfilling the no-signaling principle (see below) whose vertices are basically unknown, whereas their facets are straightforward to describe. In such case, it is thus impossible to use (A4) in order to find $\pi_V(P)$, and one needs to exploit facets of P for that purpose. A method that does the job is the Fourier-Motzkin elimination method [57], which allows one to find facets of $\pi_V(P)$ starting from facets of P.

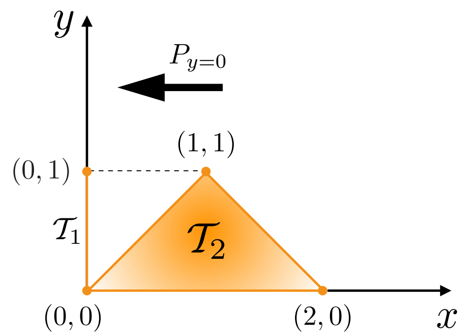

FIG. 5. Example of projection of a triangle onto the y axis. The vertices of the triangle are the set $\{(0,0),(2,0),(1,1)\}$, whose projection are the points $\{(0,0),(0,1)\}$. Therefore, the desired projected polytope is the set $0 \leqslant y \leqslant 1$.

Let us now briefly describe this method starting from an illustrative bidimensional example. Let us suppose that we want to project the triangle shown in Fig. 5 onto the y axis. It is easy to see that the inequalities defining such geometrical object are

$$x + y \leqslant 2, \quad -x + y \leqslant 0, \quad y \geqslant 0. \tag{A5}$$

If we cancel out the x coordinate from the inequalities, as we would have done when projecting vertices, we obtain the following three inequalities, $y \leqslant 2$, $y \leqslant 0$, and $y \geqslant 0$, which is not the projection we want since it defines only a single point $y = 0$. For further purposes, we notice that the result of this procedure coincides with the intersection of the polytope with the $x = 0$ axis, instead of the projection. Thus, projecting facets is a different task than projecting vertices: While for the latter it is enough to map each original vertex into the projected one, the above example shows that this procedure does not work for inequalities.

The basic principle of the Fourier-Motzkin elimination procedure is the fact that any convex combination of two facets of a polytope defines another valid inequality for it. To be more precise, let us consider a polytope $P \subset \mathbb{R}^d$ for some finite d, and let $\vec{f}_1 \cdot \vec{p} \leqslant \beta_1$ and $\vec{f}_2 \cdot \vec{p} \leqslant \beta_2$ be inequalities defining two different facets of it; here, $\vec{f}_1, \vec{f}_2 \in \mathbb{R}^d$ and $\beta_1, \beta_2 \in \mathbb{R}$, and $\vec{p} \in P$. It is clear that any vector $\vec{p}$ satisfying both these inequalities obeys also the following inequality:

$$[\lambda \vec{f}_1 + (1-\lambda)\vec{f}_2] \cdot \vec{p} \leqslant \lambda\beta_1 + (1-\lambda)\beta_2 \tag{A6}$$

for any $0 \leqslant \lambda \leqslant 1$. The Fourier-Motzkin elimination exploits this property in order to define new valid inequalities bounding the polytope in which the coordinate that we want to project out is no longer involved. Coming back to the triangle example, we notice that by taking a convex combination with $\lambda = 1/2$ of the first two inequalities in (A5) we get a new inequality that involves only y, i.e., $y \leqslant 1$. If we consider in addition the third inequality, that does not contain x, we get the right projection of the triangle, that is, the set $0 \leqslant y \leqslant 1$, as shown in Fig. 5.

Let us now state the general procedure of the Fourier-Motzkin elimination. Given a generic polytope in $\mathbb{R}^d$ defined by a finite set of inequalities $\vec{f}_i \cdot \vec{p} \leqslant \beta_i$, where $\vec{f}_i \in \mathbb{R}^d$ and $\beta_i \in \mathbb{R}$, the list of inequalities defining its projection in the subspace defined by $p_i = 0$ for some i, is obtained through the following steps:

(1) Divide the list of inequalities according to the sign of the coefficient in front of p_i to obtain three sublists $f_{i_+}, f_{i_-}, f_{i_0}$ corresponding to positive, negative, or zero coefficient.

(2) Take all the possible convex combinations between one element of f_{i_+} and one of f_{i_-}, choosing the proper combination in order to get a new valid inequality with zero coefficient in front of p_i.

(3) The obtained list, together with f_{i_0}, gives a complete set of inequalities that defines the projected polytope.

(4) Remove all the redundant inequalities to get the minimal set.

The main problem with the Fourier-Motzking elimination method is that it is in general very costly in terms of computational requirements. Indeed, due to the redundancy that one gets at each step, the time and memory needed to eliminate the variables scale exponentially with the number of variables that one wants to project out.

Another operation that we heavily exploit here is an intersection of a polytope P with a given subspace. To define it, let us consider again a linear space $\mathbb{R}^d$ and its subspace $V \subset \mathbb{R}^d$.

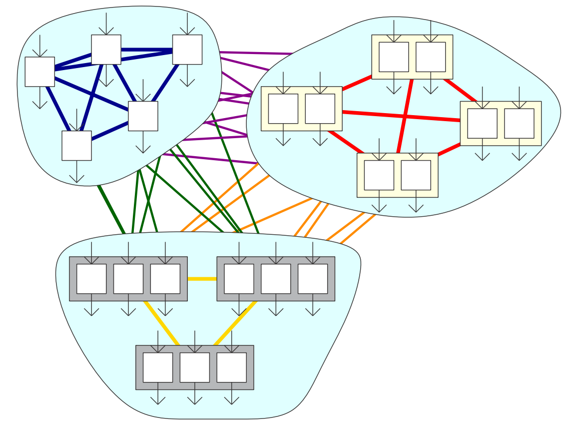

FIG. 6. An example with $N = 22$, and the 3-partition into $n_1 = 5$ sets of size 1, $n_2 = 4$ of size 2, and $n_3 = 3$ of size 3. The first sum in Eq. (B9) corresponds to the value of S_{xy} that comes from the two-body correlators $\langle M_x^{(i)} M_y^{(j)} \rangle$ within each set (i.e., $i, j \in \mathcal{A}_l$ for some l). For the 1-body boxes, these values are clearly zero, and for larger boxes, they correspond to the two-body marginals of the corresponding Popescu-Rohrlich box (PR box). Therefore, once symmetrized, the contribution of the box involving p parties using the ith strategy is $S_{xy}(p,i)$. The second sum in Eq. (B9) counts those two-body correlators $\langle M_x^{(i)} M_y^{(j)} \rangle$ in which $i \in \mathcal{A}_k$, $j \in \mathcal{A}_l$, $k \neq l$, and $|\mathcal{A}_k| = |\mathcal{A}_l| = p$. These correlations are represented by the blue, red, and yellow lines. Because they are correlations coming from different PR boxes, the locality assumption guarantees the factorization $\langle M_x^{(i)} M_y^{(j)} \rangle = \langle M_x^{(i)} \rangle \langle M_y^{(j)} \rangle$, yielding the term $S_x(p,i)S_y(p,i)$ once symmetrized. The factor $\xi_{p,i}(\xi_{p,i} - 1)$ is given by the fact that $\mathcal{S}_{xy}$ is defined as the sum for all $i \neq j$, therefore containing repetitions. Finally, the last sum in Eq. (B9) is given by all two-body correlators $\langle M_x^{(i)} M_y^{(j)} \rangle$ in which $i \in \mathcal{A}_k$, $j \in \mathcal{A}_l$, and $|\mathcal{A}_k| = p$, $|\mathcal{A}_l| = q$ with $p \neq q$, i.e., two-body correlations connecting PR boxes of different sizes. Here, the locality assumption also enables a factorization which amounts to $S_x(p,i)S_y(q,j)$ once symmetrized, weighted by the number of occurrences $\xi_{p,i}\xi_{q,j}$. These correspond to the purple, green, and orange lines in the figure.

Then, the intersection operation, denoted $\text{int}_V : \mathbb{R}^d \longrightarrow V$, is defined as

$$\text{int}_V(P) = \{\vec{x} \in P \,|\, \vec{x} \cdot \vec{w} = 0 \ \text{ for all } \ \vec{w} \in V^{\perp}\}, \tag{A7}$$

where $V^{\perp}$ is the subspace of $\mathbb{R}^d$ orthogonal to V. It is not difficult to notice that any element belonging to the intersection of P with V is also an element of its projection onto the subspace, that is,

$$\text{int}_V(P) \subseteq \pi_V(P). \tag{A8}$$

Moreover, contrary to the projection, the intersection of a polytope is more easily described in the dual representation. To show how, we define the dual basis $\{\vec{v}_i^*\}$ and $\{\vec{w}_j^*\}$ for the dual of the subspaces V and $V^{\perp}$, respectively, so to decompose any inequality in P^* as $\vec{f} = \sum_i f_i \vec{v}_i^* + \sum_j f_j \vec{w}_j^*$. Then, we can define

$$\text{int}_V(P)^* = \Big\{ g \in V^* \,|\, g = \sum_i f_i \vec{v}_i^* \quad \text{where } \ f_i = \vec{f} \cdot \vec{v}_i^* \ \text{ for } \ \vec{f} \in P^* \Big\}. \tag{A9}$$

Before moving to the application to our specific case, we also notice that (A8) implies, for the dual representation,

$$\text{int}_V(P)^* \supseteq \pi_V(P)^*, \tag{A10}$$

meaning that some inequalities valid for the intersection of the polytope might be not valid for its projection. In other words, there are generally inequalities in $\text{int}_V(P)^*$ that cannot be written as a convex combination of the original ones in P^*.

APPENDIX B: PROJECTING THE VERTICES OF THE *k*-PRODUCIBLE POLYTOPES

Here, we show in more detail how to explicitly project the vertices of the k-producible polytopes and obtain the expressions in (15) and (16). Let us start by recalling that, for any fixed L_k partition, the corresponding vertices of the $\mathcal{P}_{N,k}$ factorize in the following way:

$$p(\mathbf{a}|\mathbf{x}) = p_1(\mathbf{a}_{\mathcal{A}_1}|\mathbf{x}_{\mathcal{A}_1}) \times \cdots \times p_L(\mathbf{a}_{\mathcal{A}_L}|\mathbf{x}_{\mathcal{A}_L}), \tag{B1}$$

where each $p_s(\mathbf{a}_{\mathcal{A}_s}|\mathbf{x}_{\mathcal{A}_s})$ is a vertex of the corresponding $|\mathcal{A}_s|$-partite nonsignaling polytope. As shown in Appendix A, the vertices of the projected polytope $\mathcal{P}_{N,k}^{2,S}$ are obtained directly by projecting the original vertices into the two-body symmetric space. In other words, we simply have to compute the symmetric correlators (10) as function of (B1). Let us start by evaluating the one-body correlators as follows:

$$\begin{aligned} S_x &= \sum_{i=1}^{N} \langle M_x^{(i)} \rangle = \sum_{\mathcal{A}_s} \sum_{i \in \mathcal{A}_s} \langle M_x^{(i)} \rangle \\ &= \sum_{p=1}^{k} \sum_{\substack{\mathcal{A}_s \\ s.t. |\mathcal{A}_s| = p}} \sum_{i \in \mathcal{A}_s} \langle M_x^{(i)} \rangle \end{aligned} \tag{B2}$$

where we have first divided the summation into parties belonging to the same partition $\mathcal{A}_s$ and then further grouped the partitions of same size. Notice now that

$$\sum_{i \in \mathcal{A}_s} \langle M_x^{(i)} \rangle = \mathcal{S}_x(p_s(\mathbf{a}_{\mathcal{A}_s}|\mathbf{x}_{\mathcal{A}_s})) \tag{B3}$$

where we denote by $\mathcal{S}_x(p_s(\mathbf{a}_{\mathcal{A}_s}|\mathbf{x}_{\mathcal{A}_s}))$ the one-body components of the vector in the symmetric two-body space, obtained by projecting the vertex $p_s(\mathbf{a}_{\mathcal{A}_s}|\mathbf{x}_{\mathcal{A}_s}))$ only. Notice that the list of extremal points resulting from the projection of the vertices of the p-partite no-signaling polytope coincides with the vertices of the projected set $\mathcal{NS}_p^{2,S}$. Hence, we can rewrite (B2) as

$$S_x = \sum_{p=1}^{k} \sum_{\substack{\mathcal{A}_s \\ s.t. |\mathcal{A}_s| = p}} \mathcal{S}_x(p, i_{\mathcal{A}_s}), \tag{B4}$$

where we have now adopted the notation in (13) for the vector denoting a given vertex of the projected no-signaling polytope and $i_{\mathcal{A}_s} = 1, \ldots, n_p$ can run over all the possible choices of vertices. Now, to list all the extremal points of $\mathcal{P}_{N,k}^{2,S}$, we have to consider all the possible L_k partitions of N parties. Notice, however, that the expression in (B4) is now invariant under permutation of parties, since it is a function of the symmetric $\mathcal{S}_x$ terms only. This property allows for further simplifications: Indeed, it implies that the vertices components $\mathcal{S}_x$ are sensitive only to how many partitions of same size p are associated to the same projected vertex $\mathcal{S}_x(p, i)$, while being insensitive to which specific parties belong to such partitions. Therefore, we introduce the concept of populations $\xi_{p,i}$, which are integer numbers counting how many, among the partitions of size p, are associated to the same vertex $\mathcal{S}_x(p, i)$. Clearly, if multiplied by p, the population have to sum to the actual number of parties belonging to these partitions. Moreover, if we sum over the different sizes, we obtain the total number of particles. These conditions can be summarized by the following equation,

$$\sum_{p=1}^{k} \sum_{i=1}^{n_p} p\, \xi_{p,i} = N, \tag{B5}$$

and (B4) can now be restated as

$$S_x = \sum_{p=1}^{k} \sum_{i=1}^{n_p} \xi_{p,i} \mathcal{S}_x(p, i). \tag{B6}$$

In this formalism, running over all the choices of population satisfying (B5) corresponds to listing all the nonequivalent choices of L_k partitions.

Now that the one-body terms have been computed, we use a similar argument to compute the two-body components as function of the population and the projected components $\mathcal{S}_{xy}(p, i)$. Following from (10), we have

$$\begin{aligned} S_{xy} &= \sum_{\substack{i,\, j = 1 \\ i \neq j}}^{N} \langle M_x^{(i)} M_y^{(j)} \rangle \\ &= \sum_{\mathcal{A}_s} \sum_{\substack{i,\, j \in \mathcal{A}_s \\ i \neq j}} \langle M_x^{(i)} M_y^{(j)} \rangle + \sum_{\substack{\mathcal{A}_s,\, \mathcal{A}_t \\ s \neq t}} \langle M_x^{(i)} \rangle \langle M_y^{(j)} \rangle, \end{aligned} \tag{B7}$$

where we have used that, because of the factorization (B1), the two-body expectation values factorize as well when i, j belong to different partitions. Similar to the one-body case, we then group partitions of same sizes and substitute the sum over parties with the symmetrized correlator, so to get

$$
\begin{aligned}
S_{xy} = &\sum_{p=1}^{k} \sum_{\substack{\mathcal{A}_s \\ s.t.|\mathcal{A}_s| = p}} S_{xy}(p, i_{\mathcal{A}_s}) \\
&+ \sum_{p=1}^{k} \sum_{\substack{\mathcal{A}_s,\mathcal{A}_t \\ s.t.|\mathcal{A}_s| = |\mathcal{A}_t| = p \\ s\neq t}} S_x(p, i_{\mathcal{A}_s}) S_y(p, i_{\mathcal{A}_t}) \\
&+ \sum_{\substack{p,q=1 \\ p\neq q}}^{k} \sum_{\substack{\mathcal{A}_s,\mathcal{A}_t \\ s.t.|\mathcal{A}_s| = p \\ |\mathcal{A}_t| = q}} S_x(p, i_{\mathcal{A}_s}) S_y(q, i_{\mathcal{A}_t}).
\end{aligned} \tag{B8}
$$

Notice that we have divided the second sum in (B7) into the case where the two partitions $\mathcal{A}_s$, $\mathcal{A}_t$ are of same or different size. Lastly, we replace the sum over different vertices (B1) and all the L_k partitions with the sum over population and we arrive at

$$
\begin{aligned}
S_{xy}(\vec{\xi}) = &\sum_{p=1}^{k} \sum_{i=1}^{n_p} \xi_{p,i} S_{xy}(p, i) \\
&+ \sum_{p=1}^{k} \sum_{i=1}^{n_p} \xi_{p,i}(\xi_{p,i} - 1) S_x(p, i) S_y(p, i) \\
&+ \sum_{\{p,i\}\neq\{q,j\}} \xi_{p,i}\xi_{q,j} S_x(p, i) S_y(q, j)\,.
\end{aligned} \tag{B9}
$$

APPENDIX C: ESTIMATING THE NUMBER OF VERTICES OF $\mathcal{P}_{N,k}^{2,S}$

Here we prove that the number of vertices of $\mathcal{P}_{N,k}^{2,S}$ grows with N as $O(N^k)$.

Let $k \leqslant N$ be a constant, n_p be the number of vertices of $\mathcal{NS}_p^{2,S}$, and $n' = \max_p n_p$. Let us then define

$$
\lambda_p = p \sum_{i=1,\dots,n_p} \xi_{p,i} \tag{C1}
$$

and group the components of λ_p into a vector $\vec{\lambda}$. Observe that $\vec{\lambda}$ forms a partition of N in k elements, where the pth element is a multiple of p. Let us denote this fact as $\vec{\lambda} \vdash_k' N$. For a given p between 1 and k, we have to choose how many ways there are to partition λ_p/p into n_p possibly empty subsets. This is given by

$$
\binom{\lambda_p/p + n_p - 1}{n_p - 1} \tag{C2}
$$

ways. Therefore, the total number of partitions satisfying (14) is given by

$$
\sum_{\vec{\lambda}\vdash_k' N} \prod_{p=1}^{k} \binom{\lambda_p/p + n_p - 1}{n_p - 1}. \tag{C3}
$$

Now, we are going to give an upper bound to (C3) just to show a polynomial scaling in k. Since $\lambda_p/p \leqslant N$ and $n_p \leqslant n'$, we have the bound

$$
\begin{aligned}
\sum_{\vec{\lambda}\vdash_k' N} \prod_{p=1}^{k} \binom{\lambda_p/p + n_p - 1}{n_p - 1} &\leqslant \sum_{\vec{\lambda}\vdash_k' N} \binom{N + n' - 1}{n' - 1}^k \\
&\leqslant \binom{N + k - 1}{k - 1} \binom{N + n' - 1}{n' - 1}^k = O(N^{\zeta n' k}),
\end{aligned} \tag{C4}
$$

where $\zeta > 1$ is some constant. Note that $\binom{N+k-1}{k-1}$ counts the number of partitions of N into k possibly empty subsets, which is clearly greater than the number of partitions of N into k possibly empty subsets, satisfying the extra condition of λ_p being divisible by p. Since n' is constant because k is constant, the overall scaling is polynomial in N.

APPENDIX D: VERTICES OF THE PROJECTED NONSIGNALING POLYTOPES OF $N = 2, 3, 4$ PARTICLES

Here, we attach tables with vertices for the projections $\mathcal{NS}_N^{2,S}$ of the nonsignaling polytopes $\mathcal{NS}_N$ onto the symmetric two-body subspace for $2 \leqslant N \leqslant 4$ (Tables I–III). For completeness we also attach the table containing the deterministic values of single-body correlations (Table IV). We omit the cases $N = 5, 6$ because the lists of vertices are too long to present here.

Notice that, for the smallest Ns, the lists of vertices of the nonsignaling polytopes are known. For $N = 2$, the only nonlocal vertices belong to the equivalence class of the so-called PR

TABLE I. List of the vertices of $\mathcal{NS}_2^{2,S}$. In the first column, we also add the corresponding populations.

	S_0	S_0	S_{00}	S_{01}	S_{11}
$\xi_{2,1}$	0	0	2	2	−2
$\xi_{2,1}$	0	0	−2	2	2
$\xi_{2,3}$	0	0	2	−2	−2
$\xi_{2,4}$	0	0	−2	−2	2

TABLE II. List of the vertices of $\mathcal{NS}_3^{2,S}$. In the first column, we also add the corresponding populations.

	S_0	S_0	S_{00}	S_{01}	S_{11}
$\xi_{3,1}$	−1	−1	6	−2	−2
$\xi_{3,2}$	−1	−1	−2	−2	6
$\xi_{3,3}$	−1	1	6	2	−2
$\xi_{3,4}$	−1	1	−2	2	6
$\xi_{3,5}$	1	−1	6	2	−2
$\xi_{3,6}$	1	−1	−2	2	6
$\xi_{3,7}$	1	1	6	−2	−2
$\xi_{3,8}$	1	1	−2	−2	6

TABLE III. List of the vertices of $\mathcal{NS}_4^{2,S}$. In the first column, we also present the associated populations.

	S_0	S_0	S_{00}	S_{01}	S_{11}
$\xi_{4,1}$	-2	-2	12	0	0
$\xi_{4,2}$	-2	-2	0	0	12
$\xi_{4,3}$	-2	2	12	0	0
$\xi_{4,4}$	-2	2	0	0	12
$\xi_{4,5}$	2	-2	12	0	0
$\xi_{4,6}$	2	-2	0	0	12
$\xi_{4,7}$	2	2	12	0	0
$\xi_{4,8}$	2	2	0	0	12
$\xi_{4,9}$	0	0	12	-4	-4
$\xi_{4,10}$	0	0	-4	-4	12
$\xi_{4,11}$	0	0	12	4	-4
$\xi_{4,12}$	0	0	-4	4	12
$\xi_{4,13}$	$\frac{-20}{7}$	$\frac{-4}{7}$	$\frac{36}{7}$	$\frac{-12}{7}$	$\frac{-12}{7}$
$\xi_{4,14}$	$\frac{-20}{7}$	$\frac{-4}{7}$	$\frac{-12}{7}$	$\frac{-12}{7}$	$\frac{36}{7}$
$\xi_{4,15}$	$\frac{-20}{7}$	$\frac{4}{7}$	$\frac{36}{7}$	$\frac{12}{7}$	$\frac{-12}{7}$
$\xi_{4,16}$	$\frac{-20}{7}$	$\frac{4}{7}$	$\frac{-12}{7}$	$\frac{12}{7}$	$\frac{36}{7}$
$\xi_{4,17}$	$\frac{20}{7}$	$\frac{-4}{7}$	$\frac{36}{7}$	$\frac{12}{7}$	$\frac{-12}{7}$
$\xi_{4,18}$	$\frac{20}{7}$	$\frac{-4}{7}$	$\frac{-12}{7}$	$\frac{12}{7}$	$\frac{36}{7}$
$\xi_{4,19}$	$\frac{20}{7}$	$\frac{4}{7}$	$\frac{36}{7}$	$\frac{-12}{7}$	$\frac{-12}{7}$
$\xi_{4,20}$	$\frac{20}{7}$	$\frac{4}{7}$	$\frac{-12}{7}$	$\frac{-12}{7}$	$\frac{36}{7}$

box [32]. For $N = 3$, the list of the 46 equivalence classes was derived in Ref. [40]. Therefore, for these scenarios, the projection can be performed straightforwardly through the vertex representation (cf. Appendix A). The resulting extremal points are shown in Tables I and II in (the vertices that are shared with the local polytope are omitted). For the bipartite case, $N = 2$, the four nontrivial vertices belong obviously to a single equivalence class, corresponding to the projection of the PR box. Interestingly, there is also only one relevant class for the tripartite case, corresponding to the projection of the class number 29 of Ref. [40], which is one of the two that violate maximally the guess-your-neighbor-input inequality [58]. For higher values of N, the number of equivalence classes starts growing, as can already be seen for the vertices of $N = 4$ in Table III.

APPENDIX E: COMPLETE LIST OF FACETS FOR THE POLYTOPES THAT TEST FOR GMNL

Here, we present the complete list of facets for the polytopes that test for genuine multipartite nonlocality for $N =$ 3, 4, 5 (Tables V–VII). We omit the $N = 6, 7$ cases since the amount of inequalities starts becoming too long to be contained in one page. The inequalities are sorted in equivalence classes, under symmetry operations such as outcome-input swapping, in the same fashion as in Ref. [22].

TABLE IV. List of the values of the one- and two-body symmetric expectation values for deterministic local strategies. In this case, S_0 and S_1 contain consist of one expectation value, while S_{xy} are simply zero.

	S_0	S_1	S_{00}	S_{01}	S_{11}
$\xi_{1,1}$	1	1	0	0	0
$\xi_{1,2}$	1	-1	0	0	0
$\xi_{1,3}$	-1	1	0	0	0
$\xi_{1,4}$	-1	-1	0	0	0

TABLE V. List of the facets of the symmetric two-body polytope of two-producible correlations for $N = 3$.

β_C	α	β	γ	δ	ϵ
1	0	0	1	0	0
12	-3	1	3	$-\frac{3}{2}$	-2
6	-2	-2	0	1	0
3	0	0	0	-1	1
3	0	-2	0	0	1
3	0	0	-1	0	0

APPENDIX F: DERIVING THE INEQUALITY OF k-NONLOCALITY FOR ANY NUMBER OF PARTIES

In what follows, we explicitly compute k-producible bounds β_k [cf. Eq. (12)] for different k's for the two-body Bell expression (23). We begin with fully general considerations and later we focus on a few values of k and compute β_k case by case. Let us start by noting that, since the sets $\mathcal{P}_{N,k}^{2,S}$ are polytopes, it is enough to perform the above minimization over their vertices (see Fig. 6). Hence, by making use of Eqs. (15) and (B9), the expression $\mathcal{I}$ in Eq. (23) for all vertices of $\mathcal{P}_{N,k}^{2,S}$ can be written as

$$\begin{aligned}\mathcal{I}(\vec{S}(\vec{\xi})) = &\sum_{p=1}^{k}\sum_{i=1}^{n_p}\xi_{p,i}\mathcal{I}(\vec{S}(p,i))\\ &+\frac{1}{2}\sum_{p=1}^{k}\sum_{i=1}^{n_p}\xi_{p,i}[\xi_{p,i}-1]\mathcal{I}(\vec{S}(p,i),\vec{S}(p,i))\\ &+\frac{1}{2}\sum_{\{p,i\}\neq\{q,j\}}\xi_{p,i}\xi_{q,j}\mathcal{I}(\vec{S}(p,i),\vec{S}(q,j)),\end{aligned} \quad \text{(F1)}$$

TABLE VI. List of the facets of the symmetric two-body polytope of three-producible correlations for $N = 4$.

β_C	α	β	γ	δ	ϵ
2	1	0	1	0	0
42	12	3	6	2	-3
42	-12	9	6	-6	1
20	-5	3	4	-3	0
30	-6	3	6	-4	-1
12	0	0	3	1	-1
12	3	3	1	2	1
6	-3	0	1	0	0
8	-3	-1	2	1	0
6	0	0	1	-1	0
8	0	2	1	1	1
12	-3	-3	0	1	0
6	0	0	-1	0	0

TABLE VII. List of the facets of the symmetric two-body polytope of four-producible correlations for $N = 5$.

β_C	α	β	γ	δ	ϵ
30	−4	10	1	−2	3
40	−8	12	1	−3	3
116	28	−28	4	−9	4
134	−36	30	8	−11	4
452	−120	104	25	−37	15
562	−144	136	27	−45	22
112	28	−28	5	−9	5
116	28	−28	5	−10	5
380	−92	84	21	−34	13
36	−4	8	4	−3	2
380	−92	84	20	−33	12
320	−76	68	20	−29	10
200	−52	44	12	−17	6
16	−2	4	2	−1	1
110	−30	24	7	−9	3
20	4	−4	0	−1	0
410	−120	72	40	−30	3
170	−60	24	20	−10	1
8	0	0	2	1	0
20	0	0	3	3	1
20	−2	8	0	−1	3
20	0	4	1	−2	3
50	0	12	4	−4	5
40	−4	12	2	−3	4
80	4	12	9	−8	7
34	2	6	4	−3	3
4	2	0	1	0	0
10	−4	0	1	0	0
220	60	12	20	5	−8
120	20	−4	20	−5	−6
400	−60	36	60	−45	2
20	4	2	3	2	0
20	−4	−4	1	2	1
80	8	20	−2	5	10
40	−12	−6	5	3	0
2	0	0	0	0	1
10	0	0	−1	0	0

where we have defined the following cross terms:

$$\mathcal{I}(\vec{S}(p,i),\vec{S}(q,j)) = [S_0(p,i)+S_1(p,i)][S_0(q,j)+S_1(q,j)]. \tag{F2}$$

When the vectors $\vec{S}(p,i)$ are known, the expression (F1) takes the form of a polynomial of degree 2 in terms of the populations $\xi_{p,i}$. By grouping together the linear and quadratic terms, we get

$$\mathcal{I}(\vec{S}(\vec{\xi})) = \sum_{p=1}^{k}\sum_{i=1}^{n_p}\xi_{p,i}\big[\mathcal{I}(\vec{S}(p,i)) - \tfrac{1}{2}\mathcal{I}(\vec{S}(p,i),\vec{S}(p,i))\big] + \frac{1}{2}\sum_{p,q=1}^{k}\sum_{i,j=1}^{n_p}\xi_{p,i}\xi_{q,j}\mathcal{I}(\vec{S}(p,i),\vec{S}(q,j)). \tag{F3}$$

Then, by substituting the explicit form of the cross term (F2), one arrives at

$$\mathcal{I}(\vec{S}(\vec{\xi})) = \sum_{p=1}^{k}\sum_{i=1}^{n_p}\xi_{p,i}\big\{\mathcal{I}(\vec{S}(p,i)) - \tfrac{1}{2}[S_0(p,i)+S_1(p,i)]^2\big\} + \frac{1}{2}\left\{\sum_{p=1}^{k}\sum_{i=1}^{n_p}\xi_{p,i}[S_0(p,i)+S_1(p,i)]\right\}^2. \tag{F4}$$

With the above expression in hand, we can now seek the k-producibility bounds β_k for $\mathcal{I}$. Our approach is the following. Instead of minimizing the expression $\mathcal{I}$ for all k-producible correlations, we will rather consider a particular value of β_k and prove that the inequality $\mathcal{I} + \beta_k \geqslant 0$ holds for all integer values of $\xi_{p,i} \geqslant 0$ for $p = 1,\dots,k$ and $i = 1,\dots,n_p$ such that the condition (14) holds.

1. Cases $k = 2$ and $k = 3$

We will first consider the simplest cases of $k = 2, 3$ and show that for them $\beta_C^k = 2N$ is the correct classical bound. In other words, below we demonstrate that the following inequality,

$$2S_0 + \tfrac{1}{2}S_{00} + S_{01} + \tfrac{1}{2}S_{11} + 2N \geqslant 0, \tag{F5}$$

is satisfied for all correlations belonging to $\mathcal{P}_{N,k}^{2,S}$ for $k = 2, 3$ and any N. To this end, we use Eqs. (F4) and (14) to write down the following expression:

$$\mathcal{I}(\vec{S}(\vec{\xi})) + 2N = \sum_{p=1}^{k}\sum_{i=1}^{n_p}\xi_{p,i}\big\{\mathcal{I}(\vec{S}(p,i)) + 2p - \tfrac{1}{2}[S_0(p,i)+S_1(p,i)]^2\big\} + \frac{1}{2}\left\{\sum_{p=1}^{k}\sum_{i=1}^{n_p}\xi_{p,i}[S_0(p,i)+S_1(p,i)]\right\}^2. \tag{F6}$$

Then, plugging in the explicit values of the one- and two-body symmetric expectation values for $p = 1, 2, 3$ collected in Tables I, II, and IV, the above further rewrites as

$$\mathcal{I}(\vec{S}(\vec{\xi})) + 2N = 2[(\xi_{1,1} - \xi_{1,4} - \xi_{3,1} - \xi_{3,2} + \xi_{3,7} + \xi_{3,8})^2 + \xi_{1,1} + 2\xi_{1,2} - \xi_{1,4}] + 2[3(\xi_{2,1} + \xi_{2,2}) + \xi_{2,3} + \xi_{2,4}] + 2[(\xi_{3,1} + \xi_{3,2}) + 4(\xi_{3,3} + \xi_{3,4}) + 6(\xi_{3,5} + \xi_{3,6}) + 3(\xi_{3,7} + \xi_{3,8})]. \tag{F7}$$

With the following substitutions,

$$\begin{aligned}\mathcal{X} &= 2(\xi_{1,1} - \xi_{1,4}),\\ \mathcal{Y} &= 2(-\xi_{3,1} - \xi_{3,2} + \xi_{3,7} + \xi_{3,8}),\\ \mathcal{P}(\vec{\xi}) &= 2[\xi_{1,2} + 3(\xi_{2,1} + \xi_{2,2}) + \xi_{2,3} + \xi_{2,4} + 2(\xi_{3,1} + \xi_{3,2})\\ &\quad +4(\xi_{3,3} + \xi_{3,4}) + 6(\xi_{3,5} + \xi_{3,6}) + 2(\xi_{3,7} + \xi_{3,8})],\end{aligned} \tag{F8}$$

we can bring the expression (F7) into the following simple form:

$$\begin{aligned}\mathcal{I}(\vec{S}(\vec{\xi})) + 2N &= \tfrac{1}{2}(\mathcal{X} + \mathcal{Y})^2 + \mathcal{X} + \mathcal{Y} + \mathcal{P}(\vec{\xi})\\ &= 2\mathcal{Z}(\mathcal{Z} + 1) + \mathcal{P}(\vec{\xi}),\end{aligned} \tag{F9}$$

where $\mathcal{Z} = (\mathcal{X} + \mathcal{Y}/2)$. We then notice that all $\xi_{p,i} \geqslant 0$, which immediately implies that $\mathcal{P}(\vec{\xi}) \geqslant 0$ for all configurations of populations. Thus, we are left with the term $\mathcal{Z}(\mathcal{Z} + 1)$, which is negative only when $-1 < \mathcal{Z} < 0$. However, because $\mathcal{Z}$ is a linear combination of integers with integer coefficients, it cannot take such values. Thus, $\mathcal{Z}(\mathcal{Z} + 1) \geqslant 0$, which completes the proof.

2. The case $k = 4$

We now address the first case in which the bound β_k is different than the local bound of the Bell inequality. First of all, we notice that the bipartite nonsignaling populations $\xi_{2,i}$ enter the expression (F6) only in the linear part and, since their coefficient are always positive, we know that they never contribute to the violation of the local bound. Thus, the expression $\mathcal{I}(\vec{S}(\vec{x})) + 2N$ without these terms reads explicitly

$$\begin{aligned}&\tfrac{1}{2}(\mathcal{X} + \mathcal{Y} + \mathcal{Y}' + \mathcal{W} + \mathcal{W}')^2 + 2(\xi_{1,1} + 2\xi_{1,2} - \xi_{1,4})\\ &\quad + 2[(\xi_{3,1} + \xi_{3,2}) + 4(\xi_{3,3} + \xi_{3,4}) + 6(\xi_{3,5} + \xi_{3,6}) + 3(\xi_{3,7} + \xi_{3,8})]\\ &\quad + 2[\xi_{4,1} + \xi_{4,2} + 5(\xi_{4,3} + \xi_{4,4}) + 9(\xi_{4,5} + \xi_{4,6}) + 5(\xi_{4,7} + \xi_{4,8})]\\ &\quad + 8[\xi_{4,9} + \xi_{4,10} + 2(\xi_{4,11} + \xi_{4,12})]\\ &\quad + \tfrac{8}{49}[-22(\xi_{4,13} + \xi_{4,14}) + 19(\xi_{4,15} + \xi_{4,16}) + 89(\xi_{4,17} + \xi_{4,18}) + 48(\xi_{4,19} + \xi_{4,20})],\end{aligned} \tag{F10}$$

where $\mathcal{X}$ and $\mathcal{Y}$ are defined above and $\mathcal{Y}'$, $\mathcal{W}$, and $\mathcal{W}'$ are given by

$$\begin{aligned}\mathcal{Y}' &= 4(-\xi_{4,1} - \xi_{4,2} + \xi_{4,7} + \xi_{4,8}),\\ \mathcal{W} &= \tfrac{24}{7}(-\xi_{4,13} - \xi_{4,14} + \xi_{4,19} + \xi_{4,20}),\\ \mathcal{W}' &= \tfrac{16}{7}(-\xi_{4,15} - \xi_{4,16} + \xi_{4,17} + \xi_{4,18}).\end{aligned} \tag{F11}$$

Then, we can simplify this expression

$$\tfrac{1}{2}(\mathcal{X} + \mathcal{Y} + \mathcal{Y}' + \mathcal{W} + \mathcal{W}')^2 + \mathcal{X} + \mathcal{Y} + \mathcal{Y}' + \mathcal{W} + \mathcal{W}' + \widetilde{\mathcal{P}}(\vec{\xi}) - \tfrac{8}{49}(\xi_{4,13} + \xi_{4,14}), \tag{F12}$$

where

$$\begin{aligned}\widetilde{\mathcal{P}}(\vec{\xi}) &= 4\xi_{2,2} + 4[\xi_{3,1} + \xi_{3,2} + 2(\xi_{3,3} + \xi_{3,4}) + 3(\xi_{3,5} + \xi_{3,6}) + \xi_{3,7} + \xi_{3,8}]\\ &\quad +2[3(\xi_{4,1} + \xi_{4,2}) + 5(\xi_{4,3} + \xi_{4,4}) + 9(\xi_{4,5} + \xi_{4,6}) + 3(\xi_{4,7} + \xi_{4,8})]\\ &\quad +8[\xi_{4,9} + \xi_{4,10} + 2(\xi_{4,11} + \xi_{4,12})]\\ &\quad +\tfrac{8}{49}[33(\xi_{4,15} + \xi_{4,16}) + 75(\xi_{4,17} + \xi_{4,18}) + 27(\xi_{4,19} + \xi_{4,20})]\end{aligned} \tag{F13}$$

is a polynomial that is positive for all configurations of populations $\xi_{p,i}$. Let us now show that the expression in (F13) is always greater or equal to $-2N/49 - 1/2$. In other words, we want to prove that

$$\tfrac{1}{2}(\mathcal{X} + \mathcal{Y} + \mathcal{Y}' + \mathcal{W} + \mathcal{W}')^2 + \mathcal{X} + \mathcal{Y} + \mathcal{Y}' + \mathcal{W} + \mathcal{W}' + \widetilde{\mathcal{P}}(\vec{\xi}) - \tfrac{8}{49}(\xi_{4,13} + \xi_{4,14}) + \tfrac{1}{2} + \tfrac{2}{49}N \geqslant 0, \tag{F14}$$

for any $\xi_{p,i}$. To this end, we can exploit (14) in order to express N in terms of the populations, which allows us to see that $2N \geqslant 8(\xi_{4,13} + \xi_{4,14})$, implying that (F14) holds true. As a result, the bound for $k = 4$ amounts to

$$\beta_C^4 = \left(2 + \tfrac{2}{49}\right)N + \tfrac{1}{2}. \tag{F15}$$

3. Cases $k = 5, 6$

Based on the previous results, our guess is that for any $3 < k < N$, the bound for k-producible correlations is given by

$$\beta_C^k = 2N + \tfrac{1}{2} + \alpha_k N. \tag{F16}$$

In what follows, we estimate the correction to the linear dependence on N, that is, α_k for $k = 5, 6$, and leave the general case of any k as an open problem. To this aim, we follow the approach used in the case $k = 4$. More precisely, by substituting β_C^k given in (F16) into $\mathcal{I} + \beta_C^k$, we obtain

$$\begin{aligned}\mathcal{I}(\vec{S}(\vec{\xi})) + \beta_C^k &= \sum_{p=1}^{k}\sum_{i=1}^{n_p}\xi_{p,i}\left[\mathcal{I}(\vec{S}(p,i)) + (2+\alpha_k)p - \frac{1}{2}[S_0(p,i)+S_1(p,i)]^2\right] \\ &\quad + \frac{1}{2}\left\{\sum_{p=1}^{k}\sum_{i=1}^{n_p}\xi_{p,i}[S_0(p,i)+S_1(p,i)]\right\}^2 + \frac{1}{2} \\ &= \sum_{p=1}^{k}\sum_{i=1}^{n_p}\xi_{p,i}\Big\{\mathcal{I}_6(\vec{S}(p,i)) + (2+\alpha_k)p \\ &\quad - \frac{1}{2}[S_0(p,i)+S_1(p,i)]^2 - [S_0(p,i)+S_1(p,i)]\Big\} \\ &\quad + \frac{1}{2}\left\{\sum_{p=1}^{k}\sum_{i=1}^{n_p}\xi_{p,i}[S_0(p,i)+S_1(p,i)] + 1\right\}^2. \end{aligned} \tag{F17}$$

As the last term in this expression is always non-negative, to study the positivity of $\mathcal{I}(\vec{S}(\vec{\xi})) + \beta_C^{(k)}$, we can restrict our attention to the following function:

$$\Omega(\vec{\xi}) = \sum_{p=1}^{k}\sum_{i=1}^{n_p}\xi_{p,i}\left\{\mathcal{I}(\vec{S}(p,i)) + (2+\alpha_k)p - \frac{1}{2}[S_0(p,i)+S_1(p,i)]^2 - [S_0(p,i)+S_1(p,i)]\right\}. \tag{F18}$$

As it is a linear function in the populations which are all non-negative, its minimum is reached for the population ξ^* standing in front the expression that takes the minimal value over all choices of the vertices. In other words, we can lower bound $\Omega(\vec{x})$ as

$$\Omega(\vec{\xi}) \geqslant \xi^*(p^*\alpha_k + m_k), \tag{F19}$$

where p^* is the number of parties corresponding to x^* and m_k is defined as

$$\begin{aligned} m_k = \min_{p=1,\dots,k}\min_{i=1,\dots,n_p}\Big\{&\mathcal{I}(\vec{S}(p,i)) + 2p - \tfrac{1}{2}[S_0(p,i)+S_1(p,i)]^2 \\ &- [S_0(p,i)+S_1(p,i)]\Big\}. \end{aligned} \tag{F20}$$

Thus, we simply need to compute m_k and the value α_k we are looking for can be taken as $\alpha_k = m_k/k$ as for it $\Omega(\vec{\xi}) \geqslant 0$ for any N.

To this end, we perform the minimization in (F20) by evaluating the right-hand side on each vertex of the projected five- and six-partite no-signaling polytope. We obtain $m_5 = 40/121$ and $m_6 = 1/2$, implying that the modified bounds amount to

$$\beta_C^5 = \left(2 + \tfrac{8}{121}\right)N + \tfrac{1}{2} \tag{F21}$$

and

$$\beta_C^6 = \left(2 + \tfrac{1}{12}\right)N + \tfrac{1}{2}, \tag{F22}$$

respectively.

TABLE VIII. The local β_C, k-nonlocal β_k, quantum β_Q, and nonsignaling bounds for the Svetlichny Bell expression.

Local β_C	k-nonlocal β_k	Quantum β_Q	Nonsignaling β_{NS}
$2^{\frac{1-(-1)^N}{4}}$	$2^{(N-2\lfloor\frac{\lceil N/k\rceil}{2}\rfloor)/2}$	$2^{(N-1)/2}$	$2^{N/2}$

APPENDIX G: ESTIMATING THE SVETLICHNY AND MERMIN OPERATORS WITH COLLECTIVE SPIN MEASUREMENTS

Here, we show the details on the derivation of the witnessed for the Mermin and Svetlichny inequalities in (28) and (26). Their fully local β_C^1, the k-nonlocal $\beta_C \equiv \beta_k$, the quantum β_Q and the nonsignaling bounds are given in Tables VIII and IX.

Generally, the bounds for these inequalities are expressed in terms of the number of groups m in which the N parties are split. Noticing that N, m, and k are related by the relation $m + k - 1 \leqslant N \leqslant mk$ allows one to express the bound as a function of the nonlocality depth k (resulting in the bound in the table above). The fact that these bounds can be achieved with a model in which $\lfloor N/k \rfloor$ groups contain exactly k parties implies that the resulting bounds are tight [33]. As the quantum bound

TABLE IX. The local β_C, k-nonlocal β_k, quantum β_Q, and nonsignaling bounds for the Mermin Bell expression.

Local β_C	k-nonlocal β_k	Quantum β_Q	Nonsignaling β_{NS}
$2^{\frac{1+(-1)^N}{4}}$	$2^{(N-2\lfloor\frac{\lceil N/k\rceil+1}{2}\rfloor+1)/2}$	$2^{(N-1)/2}$	$2^{(N-1)/2}$

is larger than the $(N-1)$-nonlocal bound, the Mermin and Svetlichny expressions can reveal genuine nonlocality.

As explained in the main text, the Svetlichny and Mermin inequalities can give rise to the same witness operator:

$$\mathcal{B}_N^{\mathrm{Svet}} = \mathcal{B}_N^{\mathrm{Mermin}} = 2^{(N-1)/2}(|0\rangle\langle 1|^{\otimes N} + |1\rangle\langle 0|^{\otimes N}). \tag{G1}$$

If the mean value of this operator $\mathrm{tr}(\rho\mathcal{B}_N^{\mathrm{Svet}})$ is larger than the k-nonlocal bound given in the Table VII, we conclude that the state ρ has the capability to violate a Svetlichny inequality with the corresponding bound, that is, ρ is $(k+1)$-Bell correlated. Similarly, if the mean value of the (same) operator $\mathrm{tr}(\rho\mathcal{B}_N^{\mathrm{Mermin}})$ is larger than the k-nonlocal bound given in Table VIII, we obtain the same conclusion.

In order to state our bound in (32), we first need to prove that the following operator

$$\chi_N = |\mathrm{GHZ}_N^+\rangle\langle\mathrm{GHZ}_N^+| - |\mathrm{GHZ}_N^-\rangle\langle\mathrm{GHZ}_N^-| - \underbrace{\sigma_x^1\ldots\sigma_x^N}_{N\text{ times}} - \sum_{m\neq n}^{N}\sigma_z^m\sigma_z^n + N(N-1)\mathbb{1} \tag{G2}$$

is positive semidefinite, where $\sigma_{x/z}^i$ stands for the Pauli matrix $\sigma_{x/z}$ acting on site i. The proof can be derived in various ways from Ref. [59], focusing on genuine entanglement detection.

To this aim, let us assume for simplicity N to be even and consider the GHZ state $|\mathrm{GHZ}_N^+\rangle$, and the following set of states obtained by flipping k of its spins with $k = 1,\ldots,N/2$, that is,

$$\begin{aligned}
&\sigma_x^{i_1}|\mathrm{GHZ}^+\rangle,\\
&\sigma_x^{i_1}\sigma_x^{i_2}|\mathrm{GHZ}^+\rangle, \qquad i_1\neq i_2\\
&\vdots\\
&\sigma_x^{i_1}\sigma_x^{i_2}\ldots\sigma_x^{i_{N/2-1}}|\mathrm{GHZ}^+\rangle, \qquad i_1\neq i_2\neq\ldots\neq i_{N/2-1},\\
&\sigma_x^{i_1}\sigma_x^{i_2}\ldots\sigma_x^{i_{N/2}}|\mathrm{GHZ}^+\rangle, \qquad i_1\neq i_2\neq\ldots\neq i_{N/2},
\end{aligned} \tag{G3}$$

where $i_\ell = 1,\ldots,N$ for $\ell = 1,\ldots,N/2$. Notice that in each "line" of Eq. (G3) there are $C_N^k = \binom{N}{k}$ $(k = 1,\ldots,N/2-1)$ orthogonal states except for the last one in which the number of orthogonal vectors is $C_N^{N/2}/2$. We then construct an analogous set of vectors with $|\mathrm{GHZ}_N^-\rangle$, which altogether gives us a set of

$$2\sum_{k=0}^{N/2-1}C_N^k + C_N^{N/2} = \sum_{k=0}^{N}C_N^k = 2^N$$

orthonormal vectors forming a basis in $(\mathbb{C}^2)^{\otimes N}$. Let us now show that the operator χ_N is diagonal in this basis. For this purpose, we notice that $\sigma_x\sigma_z\sigma_x = -\sigma_z$ and therefore (see also Ref. [60])

$$\begin{aligned}
&\langle\mathrm{GHZ}_N^\pm|(\sigma_x^{i_1}\sigma_x^{i_2}\ldots\sigma_x^{i_\ell})(\sigma_z^m\sigma_z^n)(\sigma_x^{i_1}\sigma_x^{i_2}\ldots\sigma_x^{i_\ell})|\mathrm{GHZ}_N^\pm\rangle\\
&\quad = (-1)^{\lambda_{m,n}}\mathrm{tr}\big(\sigma_z^m\sigma_z^n|\mathrm{GHZ}_N^\pm\rangle\langle\mathrm{GHZ}_N^\pm|\big) = (-1)^{\lambda_{m,n}},
\end{aligned}$$

where $\ell = 1,\ldots,N/2$, $m\neq n$, and $\lambda_{m,n} = 0$ if both qubits m and n are flipped or neither of them, and $\lambda_{m,n} = -1$ if only one of them is flipped. We also notice that for the parity operator one has

$$\langle\mathrm{GHZ}_N^\pm|\big(\sigma_x^{i_1}\sigma_x^{i_2}\ldots\sigma_x^{i_\ell}\big)\big(\sigma_x^1\ldots\sigma_x^N\big)\big(\sigma_x^{i_1}\sigma_x^{i_2}\ldots\sigma_x^{i_\ell}\big)|\mathrm{GHZ}_N^\pm\rangle = \pm 1.$$

All this means that the operator χ_N is diagonal in the above basis. Furthermore, the maximal eigenvalue of $\sigma_x^1\ldots\sigma_x^N + \sum_{m\neq n}^N\sigma_z^m\sigma_z^n$ is $N(N-1)+1$ and the corresponding eigenstate is $|\mathrm{GHZ}_N^+\rangle$. Then, the other GHZ state $|\mathrm{GHZ}_N^-\rangle$ corresponds to the eigenvalue $N(N-1)-1$ and all the other elements of the above basis vectors eigenvectors with eigenvalues smaller or equal to $N(N-1)-1$. As a result, all eigenvalues of χ_N are non-negative, and hence

$$\mathcal{B}_N^{\mathrm{Svet}} = \mathcal{B}_N^{\mathrm{Mermin}} = \sqrt{2}^{N-1}(|\mathrm{GHZ}_N^+\rangle\langle\mathrm{GHZ}_N^+| - |\mathrm{GHZ}_N^-\rangle\langle\mathrm{GHZ}_N^-|) \geqslant \sqrt{2}^{N-1}\left[\sigma_x^1\ldots\sigma_x^N + \sum_{m\neq n}^N\sigma_z^m\sigma_z^n - N(N-1)\mathbb{1}\right]. \tag{G4}$$

It is not difficult to see that the same reasoning holds for odd N [in this case, the basis is formed with all possible spin flips of $(N-1)/2$ spins], and consequently the above bound is valid for any N. Noticing then that $\sum_{m\neq n}^N\sigma_z^m\sigma_z^n = 4S_z^2 + N\mathbb{1}$, where $S_z = (1/2)\sum_{i=1}^N\sigma_z^i$ is the total spin component along the z axis, we arrive at the following operator bound for the Svetlichny and Mermin Bell operators:

$$\mathcal{B}_N^{\mathrm{Svet}} = \mathcal{B}_N^{\mathrm{Mermin}} = \sqrt{2}^{N-1}(|\mathrm{GHZ}_N^+\rangle\langle\mathrm{GHZ}_N^+| - |\mathrm{GHZ}_N^-\rangle\langle\mathrm{GHZ}_N^-|) \geqslant \sqrt{2}^{N-1}\big[\sigma_x^1\ldots\sigma_x^N + 4S_z^2 - N^2\mathbb{1}\big]. \tag{G5}$$

Combining the k-nonlocal bounds of the Svetlichny and Mermin Bell expressions then allows us to write the following witness of Bell correlations depth:

$$\langle\mathcal{B}_N\rangle = \sqrt{2}^{N-1}\big\langle\sigma_x^1\ldots\sigma_x^N + 4S_z^2 - N^2\mathbb{1}\big\rangle \leqslant 2^{(N-\lceil\frac{N}{k}\rceil)/2}. \tag{G6}$$

[1] N. Brunner, D. Cavalcanti, S. Pironio, V. Scarani, and S. Wehner, Bell nonlocality, Rev. Mod. Phys. **86**, 419 (2014).

[2] A. K. Ekert, Quantum Cryptography Based on Bell's Theorem, Phys. Rev. Lett. **67**, 661 (1991).

[3] A. Acín, N. Brunner, N. Gisin, S. Massar, S. Pironio, and V. Scarani, Device-Independent Security of Quantum Cryptography Against Collective Attacks, Phys. Rev. Lett. **98**, 230501 (2007).

[4] J.-D. Bancal, N. Gisin, Y.-C. Liang, and S. Pironio, Device-Independent Witnesses of Genuine Multipartite Entanglement, Phys. Rev. Lett. **106**, 250404 (2011).

[5] Y.-C. Liang, D. Rosset, J.-D. Bancal, G. Pütz, T. J. Barnea, and N. Gisin, Family of Bell-like Inequalities as Device-Independent Witnesses for Entanglement Depth, Phys. Rev. Lett. **114**, 190401 (2015).

[6] S. Pironio, A. Acín, S. Massar, A. Boyer de la Giroday, D. N. Matsukevich, P. Maunz, S. Olmschenk, D. Hayes, L. Luo, T. A. Manning *et al.*, Random numbers certified by Bell's theorem, Nature (London) **464**, 1021 (2010).

[7] R. Colbeck, Quantum and relativistic protocols for secure multi-party computation, Ph.D. thesis, University of Cambridge, Cambridge, UK, 2007, arXiv:0911.3814; R. Colbeck and A. Kent, Private randomness expansion with untrusted devices, J. Phys. A: Math. Theor. **44**, 095305 (2011).

[8] R. Colbeck and R. Renner, Free randomness can be amplified, Nat. Phys. **8**, 450 (2012).

[9] D. Mayers and A. Yao, Self testing quantum apparatus, Quantum Inf. Comput. **4**, 273 (2004).

[10] J. S. Bell, On the Einstein Podolsky Rosen paradox, Physics **1**, 195 (1964).

[11] R. F. Werner and M. M. Wolf, All-multipartite Bell-correlation inequalities for two dichotomic observables per site, Phys. Rev. A **64**, 032112 (2001); M. Żukowski and Č. Brukner, Bell's Theorem for General N-Qubit States, Phys. Rev. Lett. **88**, 210401 (2002).

[12] B. Hensen *et al.*, Loophole-free Bell inequality violation using electron spins separated by 1.3 kilometres, Nature (London) **526**, 682 (2015).

[13] M. Giustina, M. A. M. Versteegh, S. Wengerowsky, J. Handsteiner, A. Hochrainer, K. Phelan, F. Steinlechner, J. Kofler, J. A. Larsson, C. Abellan *et al.*, Significant-Loophole-Free Test of Bell's Theorem with Entangled Photons, Phys. Rev. Lett. **115**, 250401 (2015).

[14] L. K. Shalm, E. Meyer-Scott, B. G. Christensen, P. Bierhorst, M. A. Wayne, M. J. Stevens, T. Gerrits, S. Glancy, D. R. Hamel, M. S. Allman *et al.*, Strong Loophole-Free Test of Local Realism, Phys. Rev. Lett. **115**, 250402 (2015).

[15] W. Rosenfeld, D. Burchardt, R. Garthoff, K. Redeker, N. Ortegel, M. Rau, and H. Weinfurter, Event-Ready Bell Test Using Entangled Atoms Simultaneously Closing Detection and Locality Loopholes, Phys. Rev. Lett. **119**, 010402 (2017).

[16] B. Hensen *et al.*, Loophole-free Bell test using electron spins in diamond: Second experiment and additional analysis, Sci. Rep. **6**, 30289 (2016).

[17] J. Handsteiner, A. S. Friedman, D. Rauch, J. Gallicchio, B. Liu, H. Hosp, J. Kofler, D. Bricher, M. Fink, C. Leung *et al.*, Cosmic Bell test: Measurement Settings from Milky Way Stars, Phys. Rev. Lett. **118**, 060401 (2017).

[18] J. Yin *et al.*, Satellite-based entanglement distribution over 1200 kilometers, Science **356**, 1140 (2017).

[19] The BIG Bell Test Collaboration, Challenging local realism with human choices, Nature (London) **557**, 212 (2018).

[20] D. Rauch, J. Handsteiner, A. Hochrainer, J. Gallicchio, A. S. Friedman, C. Leung, B. Liu, L. Bulla, S. Ecker, F. Steinlechner *et al.*, Cosmic Bell Test Using Random Measurement Settings from High-Redshift Quasars, Phys. Rev. Lett. **121**, 080403 (2018).

[21] M.-H. Li, C. Wu, Y. Zhang, W. Z. Liu, B. Bai, Y. Liu, W. Zhang, Q. Zhao, H. Li, Z. Wang *et al.*, Testing Local Realism into the Past Without Detection and Locality Loopholes, Phys. Rev. Lett. **121**, 080404 (2018).

[22] J. Tura, R. Augusiak, A. B. Sainz, T. Vértesi, M. Lewenstein, and A. Acín, Detecting nonlocality in many-body quantum states, Science **344**, 1256 (2014).

[23] R. Schmied, J.-D. Bancal, B. Allard, M. Fadel, V. Scarani, P. Treutlein, and N. Sangouard, Bell correlations in a Bose-Einstein condensate, Science **352**, 441 (2016).

[24] J. Tura, A. B. Sainz, T. Vértesi, A. Acín, M. Lewenstein, and R. Augusiak, Translationally invariant multipartite Bell inequalities involving only two-body correlators, J. Phys. A **47**, 424024 (2014).

[25] J. Tura, R. Augusiak, A. B. Sainz, B. Lücke, C. Klempt, M. Lewenstein, and A. Acín, Nonlocality in many-body quantum systems detected with two-body correlators, Ann. Phys. **362**, 370 (2015).

[26] J. Tura, G. de las Cuevas, R. Augusiak, M. Lewenstein, A. Acín, and I. Cirac, Energy as a Detector of Nonlocality of Many-Body Spin Systems, Phys. Rev. X **7**, 021005 (2017).

[27] S. Wagner, R. Schmied, M. Fadel, P. Treutlein, N. Sangouard, and J.-D. Bancal, Bell Correlations in a Many-Body System with Finite Statistics, Phys. Rev. Lett. **119**, 170403 (2017).

[28] K. Hammerer, A. S. Sørensen, and E. S. Polzik, Quantum interface between light and atomic ensembles, Rev. Mod. Phys. **82**, 1041 (2010).

[29] K. Eckert, O. Romero-Isart, M. Rodriguez, M. Lewenstein, E. S. Polzik, and A. Sanpera, Quantum non-demolition detection of strongly correlated systems, Nat. Phys. **4**, 50 (2008).

[30] N. J. Engelsen, R. Krishnakumar, O. Hosten, and M. A. Kasevich, Bell Correlations in Spin-Squeezed States of 500 000 Atoms, Phys. Rev. Lett. **118**, 140401 (2017).

[31] R. Augusiak, M. Demianowicz, and A. Acín, Local hidden-variable models for entangled quantum states, J. Phys. A **47**, 424002 (2014).

[32] S. Popescu and D. Rohrlich, Quantum nonlocality as an axiom, Found. Phys. **24**, 379 (1994).

[33] J.-D. Bancal, C. Branciard, N. Gisin, and S. Pironio, Quantifying Multipartite Nonlocality, Phys. Rev. Lett. **103**, 090503 (2009).

[34] F. J. Curchod, N. Gisin, and Y.-C. Liang, Quantifying multipartite nonlocality via the size of the resource, Phys. Rev. A **91**, 012121 (2015).

[35] O. Gühne, G. Tóth, and H. J. Briegel, Multipartite entanglement in spin chains, New J. Phys. **7**, 229 (2005).

[36] R. Gallego, L. E. Würflinger, A. Acín, and M. Navascués, Operational Framework for Nonlocality, Phys. Rev. Lett. **109**, 070401 (2012).

[37] J.-D. Bancal, J. Barrett, N. Gisin, and S. Pironio, Definitions of multipartite nonlocality, Phys. Rev. A **88**, 014102 (2013).

[38] A. Aloy, J. Tura, F. Baccari, A. Acín, M. Lewenstein, and R. Augusiak, Device-independent witnesses of entanglement depth from two-body correlators, arXiv:1807.06027 (unpublished).

[39] G. Svetlichny, Distinguishing three-body from two-body nonseparability by a Bell-type inequality, Phys. Rev. D **35**, 3066 (1987).

[40] S. Pironio, J.-D. Bancal, and V. Scarani, Extremal correlations of the tripartite no-signaling polytope, J. Phys. A: Math. Theor. **44**, 065303 (2011).

[41] T. Fritz, Polyhedral duality in Bell scenarios with two binary observables, J. Math. Phys. **53**, 072202 (2012).

[42] I. Pitowsky, *Quantum Probability–Quantum Logic*, Lecture Notes in Physics Vol. 321 (Springer-Verlag, Berlin, 1989).

[43] L. Babai, L. Fortnow, and C. Lund, Non-deterministic exponential time has two-prover interactive protocols, Comput. Complex. **1**, 3 (1991).

[44] J.-D. Bancal, N. Gisin, and S. Pironio, Looking for symmetric Bell inequalities, J. Phys. A: Math. Theor. **43**, 385303 (2010).

[45] M. Fadel and J. Tura, Bell correlations at finite temperature, Quantum **2**, 107 (2018).

[46] M. Fadel and J. Tura, Bounding the Set of Classical Correlations of a Many-Body System, Phys. Rev. Lett. **119**, 230402 (2017).

[47] N. D. Mermin, Simple Unified Form for the Major No-Hidden-Variables Theorems, Phys. Rev. Lett. **65**, 3373 (1990).

[48] K. Fukuda, CDD/CDD+ reference manual, ETH-Zentrum Institute for Operations Research, https://www.inf.ethz.ch/personal/fukudak/cdd_home/.

[49] X. L. Wang *et al.*, 18-Qubit Entanglement with Six Photons Three Degrees of Freedom, Phys. Rev. Lett. **120**, 260502 (2018).

[50] C. Song, K. Xu, W. Liu, C. P. Yang, S. B. Zheng, H. Deng, Q. Xie, K. Huang, Q. Guo, L. Zhang *et al.*, 10-Qubit Entanglement and Parallel Logic Operations with a Superconducting Circuit, Phys. Rev. Lett. **119**, 180511 (2017).

[51] N. Friis *et al.*, Observation of Entangled States of a Fully Controlled 20-Qubit System, Phys. Rev. X **8**, 021012 (2018).

[52] J. T. Barreiro, J.-D. Bancal, P. Schindler, D. Nigg, M. Hennrich, T. Monz, N. Gisin, and R. Blatt, Demonstration of genuine multipartite entanglement with device-independent witnesses, Nat. Phys. **9**, 559 (2013).

[53] N. D. Mermin, Extreme Quantum Entanglement in a Superposition of Macroscopically Distinct States, Phys. Rev. Lett. **65**, 1838 (1990).

[54] D. J. Wineland, J. J. Bollinger, W. M. Itano, and D. J. Heinzen, Squeezed atomic states and projection noise in spectroscopy, Phys. Rev. A **50**, 67 (1994).

[55] A. S. Sørensen and K. Mølmer, Entanglement and Extreme Spin Squeezing, Phys. Rev. Lett. **86**, 4431 (2001).

[56] A. S. Sørensen, L.-M. Duan, J. I. Cirac, and P. Zoller, Many-particle entanglement with Bose-Einstein condensates, Nature (London) **409**, 63 (2001).

[57] A. Schrijver, *Theory of Linear and Integer Programming*, Wiley-Interscience Series in Discrete Mathematics Vol. (John Wiley & Sons, New York, 1989).

[58] M. L. Almeida, J.-D. Bancal, N. Brunner, A. Acn, N. Gisin, and S. Pironio, Guess Your Neighbor's Input: A Multipartite Nonlocal Game with no Quantum Advantage, Phys. Rev. Lett. **104**, 230404 (2010).

[59] G. Toth and O. Gühne, Detecting Genuine Multipartite Entanglement with Two Local Measurements, Phys. Rev. Lett. **94**, 060501 (2005).

[60] V. Scarani and N. Gisin, Spectral decomposition of Bell's operators for qubits, J. Phys. A **34**, 6043 (2001).